Identifying the Best Machine Learning Algorithms for Brain Tumor Segmentation, Progression Assessment, and Overall Survival Prediction in the BRATS Challenge

arXiv:1811.02629v2 [cs.CV] 19 Mar 2019

Spyridon Bakas[1,2,3,†,‡,*], Mauricio Reyes[4,†], Andras Jakab[5,†,‡], Stefan Bauer[4,6,169,†], Markus Rempfler[9,65,127,†], Alessandro Crimi[7,†], Russell Takeshi Shinohara[1,8,†], Christoph Berger[9,†], Sung Min Ha[1,2,†], Martin Rozycki[1,2,†], Marcel Prastawa[10,†], Esther Alberts[9,65,127,†], Jana Lipkova[9,65,127,†], John Freymann[11,12,‡], Justin Kirby[11,12,‡], Michel Bilello[1,2,‡], Hassan M. Fathallah-Shaykh[13,‡], Roland Wiest[4,6,‡], Jan Kirschke[126,‡], Benedikt Wiestler[126,‡], Rivka Colen[14,‡], Aikaterini Kotrotsou[14,‡], Pamela Lamontagne[15,‡], Daniel Marcus[16,17,‡], Mikhail Milchenko[16,17,‡], Arash Nazeri[17,‡], Marc-Andr Weber[18,‡], Abhishek Mahajan[19,‡], Ujjwal Baid[20,‡], Elizabeth Gerstner[123,124,‡], Dongjin Kwon[1,2,†], Gagan Acharya[107], Manu Agarwal[109], Mahbubul Alam[33], Alberto Albiol[34], Antonio Albiol[34], Francisco J. Albiol[35], Varghese Alex[107], Nigel Allinson[143], Pedro H. A. Amorim[159], Abhijit Amrutkar[107], Ganesh Anand[107], Simon Andermatt[152], Tal Arbel[92], Pablo Arbelaez[134], Aaron Avery[60], Muneeza Azmat[62], Pranjal B.[107], W Bai[128], Subhashis Banerjee[36,37], Bill Barth[2], Thomas Batchelder[33], Kayhan Batmanghelich[88], Enzo Battistella[42,43], Andrew Beers[123,124], Mikhail Belyaev[137], Martin Bendszus[23], Eze Benson[38], Jose Bernal[40], Halandur Nagaraja Bharath[141], George Biros[62], Sotirios Bisdas[76], James Brown[123,124], Mariano Cabezas[40], Shilei Cao[67], Jorge M. Cardoso[76], Eric N Carver[41], Adri Casamitjana[138], Laura Silvana Castillo[134], Marcel Cat[138], Philippe Cattin[152], Albert Cérigues[40], Vinicius S. Chagas[159], Siddhartha Chandra[42], Yi-Ju Chang[45], Shiyu Chang[156], Ken Chang[123,124], Joseph Chazalon[29], Shengcong Chen[25], Wei Chen[46], Jefferson W Chen[80], Zhaolin Chen[130], Kun Cheng[120], Ahana Roy Choudhury[47], Roger Chylla[60], Albert Clrigues[40], Steven Colleman[141], Ramiro German Rodriguez Colmeiro[149,150,151], Marc Combalia[138], Anthony Costa[122], Xiaomeng Cui[115], Zhenzhen Dai[41], Lutao Dai[50], Laura Alexandra Daza[134], Eric Deutsch[43], Changxing Ding[25], Chao Dong[65], Shidu Dong[155], Wojciech Dudzik[71,72], Zach Eaton-Rosen[76], Gary Egan[130], Guilherme Escudero[159], Tho Estienne[42,43], Richard Everson[87], Jonathan Fabrizio[29], Yong Fan[1,2], Longwei Fang[54,55], Xue Feng[27], Enzo Ferrante[128], Lucas Fidon[42], Martin Fischer[95], Andrew P. French[38,39], Naomi Fridman[57], Huan Fu[90], David Fuentes[58], Yaozong Gao[68], Evan Gates[58], David Gering[60], Amir Gholami[61], Willi Gierke[95], Ben Glocker[128], Mingming Gong[88,89], Sandra Gonzlez-Vill[40], T. Grosges[151], Yuanfang Guan[108], Sheng Guo[64], Sudeep Gupta[19], Woo-Sup Han[63], Il Song Han[63], Konstantin Harmuth[95], Huiguang He[54,55,56], Aura Hernndez-Sabat[100], Evelyn Herrmann[102], Naveen Himthani[62], Winston Hsu[111], Cheyu Hsu[111], Xiaojun Hu[64], Xiaobin Hu[65], Yan Hu[66], Yifan Hu[117], Rui Hua[68,69], Teng-Yi Huang[45], Weilin Huang[64], Sabine Van Huffel[141], Quan Huo[68], Vivek HV[70], Khan M. Iftekharuddin[33], Fabian Isensee[22], Mobarakol Islam[81,82], Aaron S. Jackson[38], Sachin R. Jambawalikar[48], Andrew Jesson[92], Weijian Jian[119], Peter Jin[61], V Jeya Maria Jose[82,83], Alain Jungo[4], B Kainz[128], Konstantinos Kamnitsas[128], Po-Yu Kao[79], Ayush Karnawat[129], Thomas Kellermeier[95], Adel Kermi[74], Kurt Keutzer[61], Mohamed Tarek Khadir[75], Mahendra Khened[107], Philipp Kickingereder[23], Geena Kim[135], Nik King[60], Haley Knapp[60], Urspeter Knecht[4], Lisa Kohli[60], Deren Kong[64], Xiangmao Kong[115], Simon Koppers[32], Avinash Kori[107], Ganapathy Krishnamurthi[107], Egor Krivov[137], Piyush Kumar[47], Kaisar Kushibar[40], Dmitrii Lachinov[84,85], Tryphon Lambrou[143], Joon Lee[41], Chengen Lee[111], Yuehchou Lee[111], M Lee[128], Szidonia Lefkovits[96], Laszlo Lefkovits[97], James Levitt[62], Tengfei Li[51], Hongwei Li[65], Wenqi Li[76,77], Hongyang Li[108], Xiaochuan Li[110], Yuexiang Li[133], Heng Li[51], Zhenye Li[146], Xiaoyu Li[67], Zeju Li[158], XiaoGang Li[162], Wenqi Li[76,77], Zheng-Shen Lin[45], Fengming Lin[115], Pietro Lio[153], Chang Liu[41], Boqiang Liu[46], Xiang Liu[67], Mingyuan Liu[114], Ju Liu[115,116], Luyan Liu[112], Xavier Lladó[40], Marc

Moreno Lopez[132], Pablo Ribalta Lorenzo[72], Zhentai Lu[53], Lin Luo[31], Zhigang Luo[162], Jun Ma[73], Kai Ma[117], Thomas Mackie[60], Anant Madabushi[129], Issam Mahmoudi[74], Klaus H. Maier-Hein[22], Pradipta Maji[36], CP Mammen[161], Andreas Mang[165], B. S. Manjunath[79], Michal Marcinkiewicz[71], S McDonagh[128], Stephen McKenna[157], Richard McKinley[6], Miriam Mehl[166], Sachin Mehta[91], Raghav Mehta[92], Raphael Meier[4,6], Christoph Meinel[95], Dorit Merhof[32], Craig Meyer[27,28], Robert Miller[131], Sushmita Mitra[36], Aliasgar Moiyadi[19], David Molina-Garcia[142], Miguel A.B. Monteiro[105], Grzegorz Mrukwa[71,72], Andriy Myronenko[21], Jakub Nalepa[71,72], Thuyen Ngo[79], Dong Nie[113], Holly Ning[131], Chen Niu[67], Nicholas K Nuechterlein[91], Eric Oermann[122], Arlindo Oliveira[105,106], Diego D. C. Oliveira[159], Arnau Oliver[40], Alexander F. I. Osman[140], Yu-Nian Ou[45], Sebastien Ourselin[76], Nikos Paragios[42,44], Moo Sung Park[121], Brad Paschke[60], J. Gregory Pauloski[58], Kamlesh Pawar[130], Nick Pawlowski[128], Linmin Pei[33], Suting Peng[46], Silvio M. Pereira[159], Julian Perez-Beteta[142], Victor M. Perez-Garcia[142], Simon Pezold[152], Bao Pham[104], Ashish Phophalia[136], Gemma Piella[101], G.N. Pillai[109], Marie Piraud[65], Maxim Pisov[137], Anmol Popli[109], Michael P. Pound[38], Reza Pourreza[131], Prateek Prasanna[129], Vesna Pr?kovska[99], Tony P. Pridmore[38], Santi Puch[99], lodie Puybareau[29], Buyue Qian[67], Xu Qiao[46], Martin Rajchl[128], Swapnil Rane[19], Michael Rebsamen[4], Hongliang Ren[82], Xuhua Ren[112], Karthik Revanuru[139], Mina Rezaei[95], Oliver Rippel[32], Luis Carlos Rivera[134], Charlotte Robert[43], Bruce Rosen[123,124], Daniel Rueckert[128], Mohammed Safwan[107], Mostafa Salem[40], Joaquim Salvi[40], Irina Sanchez[138], Irina Snchez[99], Heitor M. Santos[159], Emmett Sartor[160], Dawid Schellingerhout[59], Klaudius Scheufele[166], Matthew R. Scott[64], Artur A. Scussel[159], Sara Sedlar[139], Juan Pablo Serrano-Rubio[86], N. Jon Shah[130], Nameetha Shah[139], Mazhar Shaikh[107], B. Uma Shankar[36], Zeina Shboul[33], Haipeng Shen[50], Dinggang Shen[113], Linlin Shen[133], Haocheng Shen[157], Varun Shenoy[61], Feng Shi[68], Hyung Eun Shin[121], Hai Shu[52], Diana Sima[141], M Sinclair[128], Orjan Smedby[167], James M. Snyder[41], Mohammadreza Soltaninejad[143], Guidong Song[145], Mehul Soni[107], Jean Stawiaski[78], Shashank Subramanian[62], Li Sun[30], Roger Sun[42,43], Jiawei Sun[46], Kay Sun[60], Yu Sun[69], Guoxia Sun[115], Shuang Sun[115], Yannick R Suter[4], Laszlo Szilagyi[97], Sanjay Talbar[20], Dacheng Tao[26], Dacheng Tao[90], Zhongzhao Teng[154], Siddhesh Thakur[20], Meenakshi H Thakur[19], Sameer Tharakan[62], Pallavi Tiwari[129], Guillaume Tochon[29], Tuan Tran[103], Yuhsiang M. Tsai[111], Kuan-Lun Tseng[111], Tran Anh Tuan[103], Vadim Turlapov[85], Nicholas Tustison[28], Maria Vakalopoulou[42,43], Sergi Valverde[40], Rami Vanguri[48,49], Evgeny Vasiliev[85], Jonathan Ventura[132], Luis Vera[142], Tom Vercauteren[76,77], C. A. Verrastro[149,150], Lasitha Vidyaratne[33], Veronica Vilaplana[138], Ajeet Vivekanandan[60], Guotai Wang[76,77], Qian Wang[112], Chiatse J. Wang[111], Weichung Wang[111], Duo Wang[153], Ruixuan Wang[157], Yuanyuan Wang[158], Chunliang Wang[167], Guotai Wang[76,77], Ning Wen[41], Xin Wen[67], Leon Weninger[32], Wolfgang Wick[24], Shaocheng Wu[108], Qiang Wu[115,116], Yihong Wu[144], Yong Xia[66], Yanwu Xu[88], Xiaowen Xu[115], Peiyuan Xu[117], Tsai-Ling Yang[45], Xiaoping Yang[73], Hao-Yu Yang[93,94], Junlin Yang[93], Haojin Yang[95], Guang Yang[143], Hongdou Yao[98], Xujiong Ye[143], Changchang Yin[67], Brett Young-Moxon[60], Jinhua Yu[158], Xiangyu Yue[61], Songtao Zhang[30], Angela Zhang[79], Kun Zhang[90], Xuejie Zhang[98], Lichi Zhang[112], Xiaoyue Zhang[118], Yazhuo Zhang[145,146,147], Lei Zhang[143], Jianguo Zhang[157], Xiang Zhang[162], Tianhao Zhang[168], Sicheng Zhao[61], Yu Zhao[65], Xiaomei Zhao[144,55], Liang Zhao[163,164], Yefeng Zheng[117], Liming Zhong[53], Chenhong Zhou[25], Xiaobing Zhou[98], Fan Zhou[51], Hongtu Zhu[51], Jin Zhu[153], Ying Zhuge[131], Weiwei Zong[41], Jayashree Kalpathy-Cramer[123,124,†], Keyvan Farahani[12,†,‡], Christos Davatzikos[1,2,†,‡], Koen van Leemput[123,124,125,†], and Bjoern Menze[9,65,127,†,*]

[1] Center for Biomedical Image Computing and Analytics, University of Pennsylvania, Philadelphia, PA, USA
[2] Department of Radiology, Perelman School of Medicine, University of Pennsylvania, Philadelphia, PA, USA
[3] Department of Pathology and Laboratory Medicine, Perelman School of Medicine, University of Pennsylvania, Philadelphia, PA, USA
[4] Institute for Surgical Technology and Biomechanics, University of Bern, Bern, Switzerland

[5] Center for MR-Research, University Children's Hospital Zurich, Zurich, Switzerland
[6] Support Centre for Advanced Neuroimaging Inselspital, Institute for Diagnostic and Interventional Neuroradiology, Bern University Hospital, Bern, Switzerland
[7] University Hospital of Zurich, Zurich, Switzerland
[8] Center for Clinical Epidemiology and Biostatistics, University of Pennsylvania, Philadelphia, USA
[9] Image-Based Biomedical Modeling Group, Technical University of Munich, Munich, Germany
[10] Icahn School of Medicine, Mount Sinai Health System, New York, NY, USA
[11] Leidos Biomedical Research, Inc., Frederick National Laboratory for Cancer Research, Frederick, MD 21701, USA
[12] Cancer Imaging Program, National Cancer Institute, National Institutes of Health, Bethesda, MD 20814, USA
[13] Department of Neurology, The University of Alabama at Birmingham, Birmingham, AL, USA
[14] Department of Diagnostic Radiology, University of Texas MD Anderson Cancer Center, Houston, TX, USA
[15] Department of Psychology, Washington University, St. Louis, MO, USA
[16] Neuroimaging Informatics and Analysis Center, Washington University, St. Louis, MO, USA
[17] Department of Radiology, Washington University, St. Louis, MO, USA
[18] Institute of Diagnostic and Interventional Radiology, Pediatric Radiology and Neuroradiology, University Medical Center Rostock, Ernst-Heydemann-Str. 6, 18057 Rostock, Germany
[19] Tata Memorial Centre, Homi Bhabha National Institute, Mumbai, India
[20] Shri Guru Gobind Singhji Institute of Engineering and Technology, Nanded, India
[21] NVIDIA, Santa Clara, USA
[22] Division of Medical Image Computing, German Cancer Research Center (DKFZ), Heidelberg, Germany
[23] Department of Neuroradiology, University of Heidelberg Medical Center, Heidelberg, Germany
[24] Neurology Clinic, University of Heidelberg Medical Center, Heidelberg, Germany
[25] School of Electronic and Information Engineering, South China University of Technology, Guangzhou, China
[26] UBTECH Sydney AI Centre, SIT, FEIT, University of Sydney, Sydney, Australia
[27] Biomedical Engineering, University of Virginia, Charlottesville, VA 22903, USA
[28] Radiology and Medical Imaging, University of Virginia, Charlottesville, VA 22903, USA
[29] EPITA Research and Development Laboratory (LRDE), France
[30] Southern University of Science and Technology, Shenzhen, China
[31] Peking University, China
[32] Institute of Imaging and Computer Vision, RWTH Aachen University, Aachen, Germany
[33] Vision Lab, Electrical and Computer Engineering, Old Dominion University, Norfolk, VA, USA
[34] iTeam, Universitat Politecnica Valencia, Spain
[35] Instituto de Fisica Corpuscular, Universitat de Valencia, Consejo Superior de Investigaciones Cientificas, Spain
[36] Machine Intelligence Unit, Indian Statistical Institute, Kolkata, 700108, India
[37] Department of CSE, University of Calcutta, Kolkata, India
[38] Computer Vision Lab, School of Computer Science, University of Nottingham, Nottingham, UK
[39] School of Biosciences, University of Nottingham, Nottingham, UK
[40] Research Institute of Computer Vision and Robotics, University of Girona, Spain
[41] Henry Ford Health System, Detroit, MI, USA
[42] CVN, CentraleSuplec, Universit Paris-Saclay, France
[43] Gustave Roussy Institute, France
[44] TheraPanacea, France
[45] Department of Electrical Engineering, National Taiwan University of Science and Technology, Taipei, Taiwan
[46] Dept. of Biomedical Engineering, School of Control Science and Engineering, Shandong University, China
[47] Department of Computer Science, Florida State University, Tallahassee, FL, USA
[48] Department of Radiology, Columbia University Medical Center, New York, NY, USA
[49] Data Science Institute, Columbia University, New York, NY, USA
[50] Faculty of Business and Economics, The University of Hong Kong, Hong Kong
[51] Department of Biostatistics, University of North Carolina, Chapel Hill, NC, USA
[52] Department of Biostatistics, University of Texas, MD Anderson Cancer Center, Houston, TX, USA
[53] Southern Medical University, Guangzhou, China
[54] Research Center for Brain-inspired Intelligence, Institute of Automation, Chinese Academy of Sciences, China
[55] University of Chinese Academy of Sciences, China
[56] Center for Excellence in Brain Science and Intelligence Technology, Chinese Academy of Sciences, China
[57] Afeka Academic College of Engineering, Tel Aviv, Israel
[58] Department of Imaging Physics, University of Texas MD Anderson Cancer Center, Houston, TX, USA
[59] Department of Cancer Systems Imaging and Diagnostic Radiology, University of Texas MD Anderson Cancer Center, Houston, TX, USA
[60] HealthMyne, Madison, WI, USA

[61] University of California, Berkeley, CA, USA
[62] Institute for Computational Engineering and Science, University of Texas, Austin, TX, USA
[63] Odiga London, London, UK
[64] Malong Tehnologies, China
[65] Department of Computer Science, Technical University of Munich, Munich, Germany
[66] School of Computer Science and Engineering, Northwestern Polytechnical University, University of Xian, Xian 710072, China
[67] The First Affiliated Hospital of Xi'an Jiao Tong University, Peoples Republic of China, China
[68] Shanghai United Imaging Intelligence Co., Ltd, Shanghai, China
[69] School of Biomedical Engineering, Southeast University, Nanjing, China
[70] Harvard University, Cambidge, MA, USA
[71] Future Processing, Poland
[72] Silesian University of Technology, Gliwice, Poland
[73] Department of Mathematics, Nanjing University of Science and Technology, China
[74] LMCS Laboratory, National Higher School of Computer Sciences (ESI), Algeria
[75] LabGed Laboratory, Dept. of Computer Sciences, University Badji-Mokhtar of Annaba, Algeria
[76] School of Biomedical Engineering and Imaging Sciences, King's College London, London, UK
[77] Wellcome / EPSRC Centre for Interventional and Surgical Sciences, University College London, London, UK
[78] Stryker Corporation, Navigation. Freiburg im Breisgau, Germany.
[79] Vision Research Lab, University of California, Santa Barbara, CA, USA
[80] UC Irvine Health, University of California, Irvine, CA, USA
[81] Graduate School for Integrative Sciences and Engineering, National University of Singapore, Singapore
[82] Department of Biomedical Engineering, National University of Singapore, Singapore
[83] Dept. of Instrumentation and Control Engineering, National Institute of Technology, Tiruchirappalli, India
[84] Intel, Nizhny Novgorod, Russian Federation
[85] Lobachevsky State University, Russian Federation
[86] Technological Institute of Irapuato, Information Technologies Laboratory, Mexico
[87] College of Engineering, Mathematics and Physical Sciences, University of Exeter, UK
[88] Department of Biomedical Informatics, University of Pittsburgh, PA, USA
[89] Philosophy Department, Carnegie Mellon University, Pittsburgh, PA, USA
[90] UBTECH Sydney AI Centre, SIT, FEIT, The University of Sydney, Australia
[91] University of Washington, Seattle, WA, USA
[92] Centre for Intelligent Machines (CIM), McGill University, Montreal, QC, Canada
[93] Yale University, New Haven, CT, USA
[94] Cura Cloud Cooperation, Seattle, WA, USA
[95] Hasso-Plattner Institute for Digital Engineering, Prof.-Dr.-Helmert-Strae 2-3, 14482 Potsdam, Germany
[96] Department of Computer Science, University of Medicine, Pharmacy, Sciences and Technology, Romania
[97] Department of Electrical Engineering, Sapientia Hungarian University of Transylvania, Romania
[98] School of Information Science and Engineering, Yunnan University, P.R.China
[99] QMENTA, Boston, MA, USA
[100] Computer Vision Center, Universitat Autonoma de Barcelona, Spain
[101] SIMBIOsys, Universitat Pompeu Fabra, Spain
[102] University Clinic for Radio-oncology, Bern University Hospital, Switzerland
[103] Faculty of Math and Computer Science, University of Science, Vietnam National University, Vietnam
[104] Department of Computer Science, Sai Gon University, Vietnam
[105] INESC-ID, Portugal
[106] Instituto Superior Tecnico, Portugal
[107] Indian Institute of Technology Madras, Chennai, India
[108] University of Michigan, Ann Arbor, MI, USA
[109] Indian Institute of Technology Roorkee, India
[110] Tianjin University, China
[111] National Taiwan University, Taiwan
[112] School of Biomedical Engineering, Shanghai Jiao Tong University, China
[113] School of Biomedical Engineering, Shanghai Jiao Tong University, China
[114] Department of biological science and medical engineering, Beihang University, China
[115] School of Information Science and Engineering, Shandong University, China
[116] Institute of Brain and Brain-Inspired Science, Shandong University, China
[117] Tencent Youtu Lab, China
[118] QED Technologies. Co., Ltd, China

[119] Beihang University, China
[120] Beijing University of Posts and Telecommunications University, China
[121] Deepnoid, South Korea
[122] Department of Neurosurgery, Mount Sinai Health System, New York, NY, USA
[123] Athinoula A Martinos Center for Biomedical Imaging, Massachusetts General Hospital, Boston, MA, USA
[124] Department of Radiology, Harvard Medical School, Harvard University, Boston, MA, USA
[125] Department of Applied Mathematics and Computer Science, Technical University of Denmark, Denmark
[126] Department of Neuroradiology, Technical University of Munich, Munich, Germany
[127] Institute for Biomedical Engineering, Technical University of Munich, Munich, Germany
[128] Biomedical Image Analysis Group, Imperial College London, London, UK
[129] Case Western Reserve University, Cleveland OH 44106, USA
[130] Monash Biomedical Imaging, Monash University, Melbourne, Australia
[131] Radiation Oncology Branch, National Cancer Institute, National Institutes of Health, Bethesda, MD 20814, USA
[132] Department of Computer Science, University of Colorado, Colorado Springs, CO, USA
[133] College of Computer Science and Software Engineering, Computer Vision Institute, Shenzhen University, Shenzhen, China
[134] Department of Biomedical Engineering, Universidad de los Andes, Bogota, Colombia
[135] College of Computer and Information Sciences, Regis University, Denver, CO, USA
[136] Indian Institute of Information Technology, Vadodara, Gandhinagar Campus, Vadodara 382028, Gujarat, India
[137] Kharkevich Institute for Information Transmission Problems, Moscow, Russia
[138] Signal Theory and Communications Department, Universitat Politecnica de Catalunya - BarcelonaTech, Barcelona, Spain
[139] Independent research, No Institutional Affiliation
[140] Radiation Oncology Department, American University of Beirut Medical Center, Beirut 1107 2020, Riad El-Solh, Lebanon
[141] Department of Electrical Engineering (ESAT), STADIUS Center for Dynamical Systems, Signal Processing and Data Analytics, KU Leuven, Leuven, Belgium
[142] Mathematical Oncology Laboratory, Universidad de Castilla-La Mancha, Ciudad Real, Spain
[143] University of Lincoln, Lincoln, LN6 7TS, UK
[144] National Laboratory of Pattern Recognition, Institute of Automation, Chinese Academy of Sciences, Beijing, China
[145] Beijing Neurosurgical Institute, Capital Medical University, Beijing, China
[146] Department of Neurosurgery, Beijing Tiantan Hospital, Capital Medical University, Beijing, China
[147] Beijing Institute for Brain Disorders Brain Tumor Center, Beijing, China
[148] China National Clinical Research Center for Neurological Diseases, Beijing, China
[149] Universidad Tecnologica Nacional, Buenos Aires, Argentina
[150] Comision Nacional de Energia Atomica, Buenos Aires, Argentina
[151] GAMMA3 (UTT-INRIA), ICD-UMR CNRS 6281, University of Technology of Troyes, Troyes, France
[152] Department of Biomedical Engineering, University of Basel, Switzerland
[153] Computer Laboratory, University of Cambridge, Cambridge, CB3 0FD, UK
[154] Department of Radiology, University of Cambridge, Cambridge, CB2 0QQ, UK
[155] Computer Science and Engineer College, Chongqing University of Technology, China, 40054
[156] IBM T. J. Watson Research, Yorktown Height, NY 10598, USA
[157] Computing, School of Science and Engineering, University of Dundee, Dundee, UK
[158] Department of Electronic Engineering, Fudan University, Shanghai, China
[159] Hospital Israelita Albert Einstein, So Paulo, Brazil
[160] Massachusetts General Hospital, Boston, MA, USA
[161] NVIDIA, India
[162] National University of Defense Technology, Changsha 410073, China
[163] Siemens, USA
[164] State University of New York at Buffalo, Buffalo, NY, USA
[165] Department of Mathematics, College of Natural Sciences and Mathematics, University of Houston, Houston, TX, USA
[166] Department of Computer Science, University of Stuttgart
[167] School for Technology and Health (STH), KTH Royal institute of technology, SE-14152 Huddinge, Stockholm, Sweden
[168] General Electric, USA
[169] Helbling Technik AG, Bern, Switzerland

†: People involved in the organization of the challenge

‡: People contributing data from their institutions
* Corresponding authors: s.bakas@uphs.upenn.edu, bjoern.menze@tum.de

Abstract. Gliomas are the most common primary brain malignancies, with different degrees of aggressiveness, variable prognosis and various heterogeneous histologic sub-regions, i.e., peritumoral edematous/invaded tissue, necrotic core, active and non-enhancing core. This intrinsic heterogeneity is also portrayed in their radio-phenotype, as their sub-regions are depicted by varying intensity profiles disseminated across multi-parametric magnetic resonance imaging (mpMRI) scans, reflecting varying biological properties. Their heterogeneous shape, extent, and location are some of the factors that make these tumors difficult to resect, and in some cases inoperable. The amount of resected tumor is a factor also considered in longitudinal scans, when evaluating the apparent tumor for potential diagnosis of progression. Furthermore, there is mounting evidence that accurate segmentation of the various tumor sub-regions can offer the basis for quantitative image analysis towards prediction of patient overall survival. This study assesses the state-of-the-art machine learning (ML) methods used for brain tumor image analysis in mpMRI scans, during the last seven instances of the International Brain Tumor Segmentation (BraTS) challenge, i.e., 2012-2018. Specifically, we focus on i) evaluating segmentations of the various glioma sub-regions in pre-operative mpMRI scans, ii) assessing potential tumor progression by virtue of longitudinal growth of tumor sub-regions, beyond use of the RECIST/RANO criteria, and iii) predicting the overall survival from pre-operative mpMRI scans of patients that underwent gross total resection. Finally, we investigate the challenge of identifying the best ML algorithms for each of these tasks, considering that apart from being diverse on each instance of the challenge, the multi-institutional mpMRI BraTS dataset has also been a continuously evolving/growing dataset.

Keywords: BraTS, challenge, brain, tumor, segmentation, machine learning, glioma, glioblastoma, radiomics, survival, progression, RECIST, RANO

1 Introduction

1.1 Scope

The Brain Tumor segmentation (BraTS) challenge focuses on the evaluation of state-of-the-art methods for the segmentation of brain tumors in multi-parametric magnetic resonance imaging (mpMRI) scans. Its primary role since its inception has been two-fold: a) a publicly available dataset and b) a community benchmark [1–4]. BraTS utilizes multi-institutional pre-operative mpMRI scans and focuses on the segmentation of intrinsically heterogeneous (in appearance, shape, and histology) brain tumors, namely gliomas. Furthermore, to pinpoint the clinical relevance of this segmentation task, BraTS 2018 also focuses on the prediction of patient overall survival, via integrative analyses of radiomic features and machine learning (ML) algorithms.

1.2 Clinical Relevance

Gliomas are the most common primary brain malignancies, with different degrees of aggressiveness, variable prognosis and various heterogeneous histological sub-regions, i.e., peritumoral edematous/invaded tissue, necrotic core, active and non-enhancing core. This intrinsic heterogeneity of gliomas is also portrayed in their imaging phenotype (appearance and shape), as their sub-regions are described by varying intensity profiles disseminated across mpMRI scans, reflecting varying tumor biological properties. Due to this highly heterogeneous appearance and shape, segmentation of brain tumors in multimodal MRI scans is one of the most challenging tasks in medical image analysis.

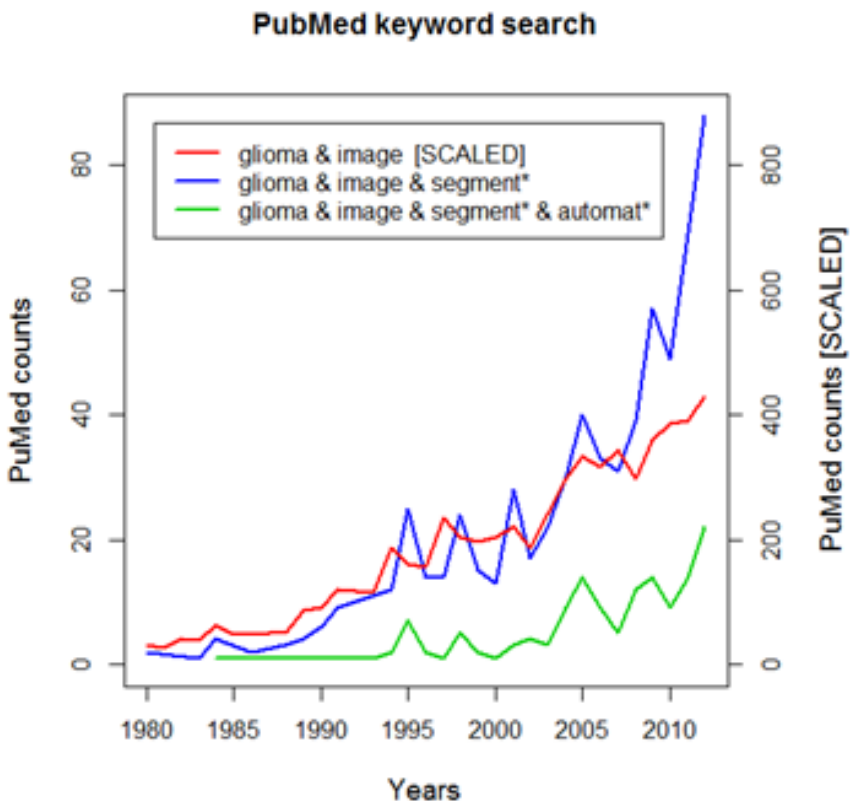

Fig. 1: Search on PubMed in 2012 showing related growing body of literature. Figure taken from [1].

1.3 Before the BraTS era

There has been a growing body of literature on computational algorithms addressing this important task (Fig. 1). Unfortunately, open manually-annotated datasets for designing and testing these algorithms are not currently available, and private datasets differ so widely that it is hard to compare the different segmentation strategies that have been reported so far. Critical factors leading to these differences include, but are not limited to, i) the imaging modalities employed, ii) the type of the tumor (glioblastoma or lower grade glioma, primary or secondary tumors, solid or infiltratively growing), and iii) the state of disease (images may not only be acquired prior to treatment, but also post-operatively and therefore show radiotherapy effects and surgically-imposed cavities). Towards this end, BraTS is making available a large dataset of mpMRI [1–4], with accompanying delineations of the relevant tumor sub-regions (Fig. 2). The exact mpMRI data consists of a) a native T1-weighted scan (T1), b) a post-contrast T1-weighted scan (T1Gd), c) a native T2-weighted scan (T2), and d) a T2 Fluid Attenuated Inversion Recovery (T2-FLAIR) scan.

1.4 BraTS 2017 vs 2018

The last two instances of BraTS (i.e., 2017 and 2018) were focused on both the segmentation of tumor sub-structures, and the prediction of overall survival of patients diagnosed with primary de novo glioblastoma (GBM).

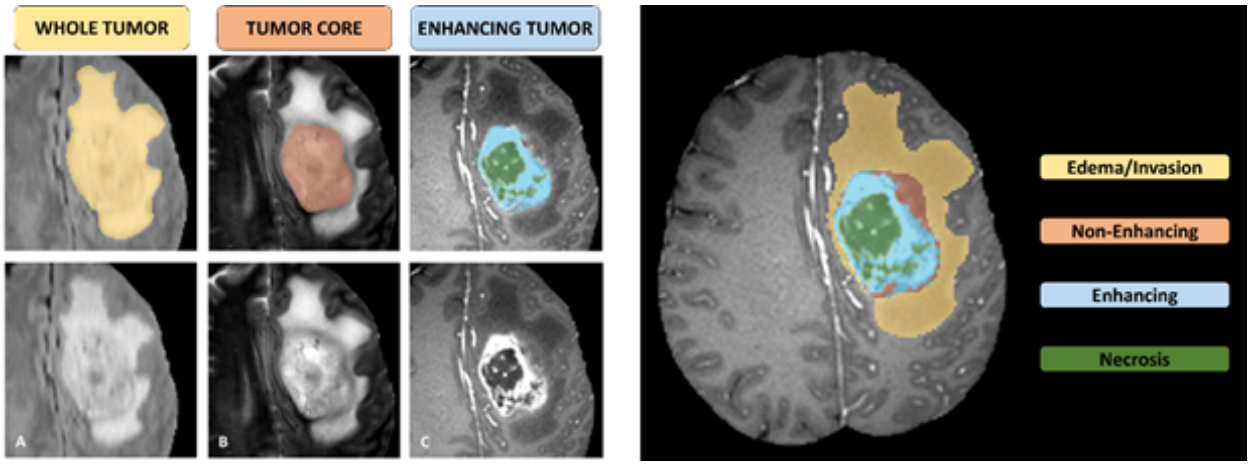

Fig. 2: Glioma sub-regions. The image patches show from left to right: the whole tumor (yellow) visible in T2-FLAIR (A), the tumor core (red) visible in T2 (B), the active tumor structures (light blue) visible in T1Gd, surrounding the cystic/necrotic components of the core (green) (C). The segmentations are combined to generate the final labels of the tumor sub-regions (D): ED (yellow), NET (red), NCR cores (green), AT (blue). Figure taken from [1].

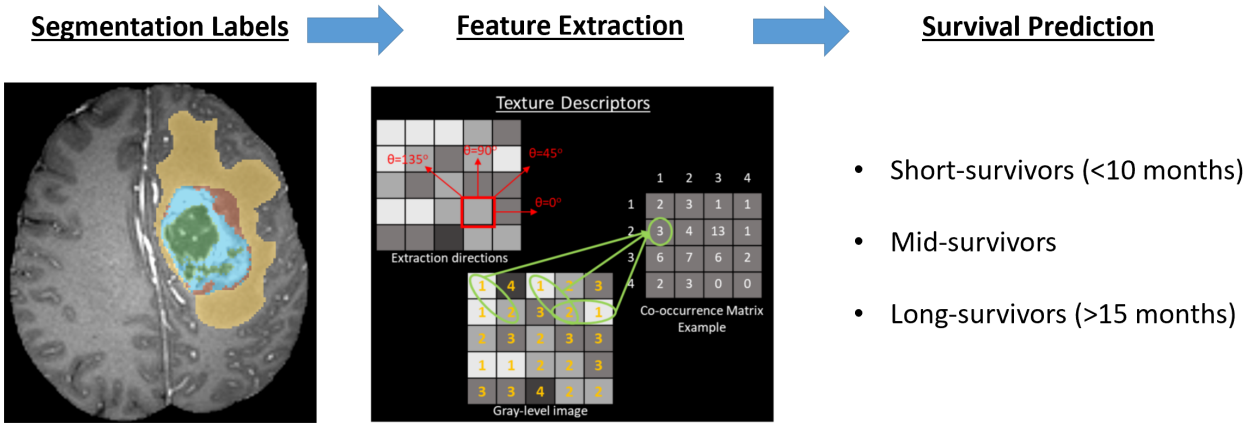

Fig. 3: Illustrative pipeline example for predicting patient overall survival.

For the segmentation of gliomas in pre-operative mpMRI scans, the participants were called to address this task by using the provided clinically-acquired training data to develop automated methods and produce segmentation labels of the different glioma sub-regions.

For the task of patient overall survival (OS) prediction from pre-operative mpMRI scans, once the participants produce their segmentation labels in the pre-operative scans, they were called to use these labels in combination with the provided mpMRI data to extract imaging/radiomic features that they consider appropriate [5], and analyze them through ML algorithms, to predict patient OS (Fig. 3). The participants do not need to be limited to volumetric parameters, but can also consider intensity, morphologic, histogram-based, and textural features, as well as spatial information, and glioma diffusion properties extracted from glioma growth models.

2 Materials and Methods

Table 1: Summarizing the original characteristics of the BraTS dataset.

Acronym	MRI Sequence	Property	Acquisition	Slice thickness
T1	T1-weighted	Native image	Sagittal or Axial	Variable (1-5mm)
T1Gd	T1-weighted	post-contrast enhancement (Gadolinium)	Axial 3D acquisition	Variable
T2	T2-weighted	Native image	Axial 2D	Variable (2-4mm)
T2-FLAIR	T2-weighted	Native image	Axial or Coronal or Sagittal 2D	Variable

2.1 BraTS Annotations and Structures

All the imaging datasets have been segmented manually, by one to four raters, following the same annotation protocol, and their ground truth annotations were approved by experienced neuro-radiologists. The tumor sub-regions considered for evaluation are: 1) the "active tumor" (AT), 2) the gross tumor, also known as the "tumor core" (TC), and 3) the complete tumor extent also referred to as the "whole tumor" (WT) (Fig. 2). The AT is described by areas that show hyper-intensity in T1Gd when compared to T1, but also when compared to "healthy" white matter in T1Gd. The TC describes the bulk of the tumor, which is what is typically resected. The TC entails the AT, as well as the necrotic (fluid-filled) and the non-enhancing (solid) parts of the tumor. The appearance of the necrotic (NCR) and the non-enhancing (NET) tumor core is typically hypo-intense in T1-Gd when compared to T1. The WT describes the complete extent of the disease, as it entails the TC and the peritumoral edematous/invaded tissue (ED), which is typically depicted by hyper-intense signal in T2-FLAIR.

The ground truth annotations were only approved by domain experts whereas they are actually created by multiple experts. Although a very specific annotation protocol (described below) was provided to each data contributing institution, slightly different annotation styles were noted for the various raters involved in the process. Therefore, all final labels included in the BraTS dataset were also further reviewed for consistency and compliance with the annotation protocol by a single board-certified neuro-radiologist with more than 15 years of experience.

2.2 Annotation Protocol

The BraTS dataset describes a collection of brain tumor MRI scans acquired from multiple different centers under standard clinical conditions, but with different equipment and imaging protocols, resulting in a vastly heterogeneous image quality reflecting diverse clinical practice across different institutions. However, we designed the following tumor annotation protocol, in order to make it possible to create similar ground truth delineations across various annotators.

For the tasks related to BraTS, only structural MRI volumes were considered (T1, T1Gd, T2, T2-FLAIR), all of them co-registered to a common anatomical template (SRI [6]) and resampled to $1mm^3$. The details of the original scans are given in Table 1. Note that different native T1 scans exist, depending on whether they were 3D acquisitions, or 2D fast spin echo, or even just localizing images, and therefore not all T1 scans can be considered suitable for the task of segmentation. To our experience the T1Gd and the T2-FLAIR volumes have been the most useful to produce the ground truth segmentations.

We note that radiologic definition of tumor boundaries, especially in such infiltrative tumors as gliomas, is a well-known problem. In an attempt to offer a standardized approach to assess and evaluate various tumor sub-regions, the BraTS initiative, after consultation with internationally-recognized expert neuroradiologists, defined the following types of tumor sub-regions. However, we note that other criteria for delineation could be set, resulting in slightly different tumor sub-regions. The BraTS tumor sub-regions do not reflect strict biologic entities, but are rather image-based.

For instance, the definition of the AT could simply be the regions with hyper-intense signal on T1Gd images. However, in high grade tumors, there are non-necrotic, non-cystic regions that do not enhance, but can be separable from the surrounding vasogenic edema, and represent non-enhancing infiltrative tumor. Another problem is the definition of tumor center in low-grade gliomas. In such cases, it is difficult to differentiate tumor from vasogenic edema, particularly in the absence of enhancement. It is also noteworthy that in order to produce the ground truth labels used in the provided data, we have recommended to start delineating the sub-regions of interest from the outside tumor boundaries, i.e., one should start from the manual delineation of the abnormal signal in the T2-weighted images, primarily defining the WT, then address the TC, and finally the enhancing and non-enhancing/necrotic core, possibly using semi-automatic tools.

2.2.1 BraTS 2012-2016 (Four tumor sub-regions) BraTS 2012-2016 defined four tumor sub-regions, delineating the AT, NET, NCR, and ED.

Label 1: NCR. This sub-region describes the necrotic core, or necrocyst, that resides within the enhancing rim of high grade gliomas, and sometimes appears cystic.

Label 2: ED. This sub-region describes the peritumoral edematous and invaded tissue that is fairly easily defined on the T2-weighted images, as a hyperintense abnormal signal distribution, and hypo-intense signal on T1. This label primarily describes the tentacle-like shaped regions of edematous white matter into the subcortex of the gyri and, importantly, this is distinguished from cystic regions and the ventricles.

Label 3: NET. It is possible to identify such regions depicting the non-enhancing gross abnormality, by viewing the T2-weighted images. Some parts of the high-grade tumor do not enhance, but they are clearly distinguishable from the surrounding vasogenic edema on T2, as they have lower signal intensity and heterogeneous texture. Moreover, in low grade gliomas, this is the only category used for delineating the gross tumor.

Label 4: AT. This is a relatively easy definition, as it describes the enhancing regions within the gross tumor abnormality, but not the necrotic center. The threshold to exclude the necrotic center from the enhancing part should be set independently per subject. Note that vessels running in the neighboring regions and sulci are not included.

We cautiously note that the NET (i.e., ”Label 3”) can be overestimated by some annotators, and that oftentimes there is little evidence in the image data for this sub-region. Therefore, forcing the definition of this region could introduce an artifact, which could result in substantially different ground truth labels created from the annotators in different institutions. This case could potentially have implications in the ranking of the BraTS participants, i.e., a ranking bias towards the test cases ground truth annotator instead of ranking the actual algorithmic performance.

2.2.2 BraTS 2017-Present (Three tumor sub-regions) In order to address the aforementioned issue, in BraTS 2017 the NET label (”Label 3”) has been eliminated and combined with NCR (”Label 1”). Furthermore, contralateral and periventricular regions of T2-FLAIR hyper-intensity were excluded from the ED region, unless they were contiguous with peritumoral ED, as these areas are generally considered to represent chronic microvascular changes, or age-associated demyelination, rather than tumor infiltration [7]. The rationale for this is that contralateral and periventricular white matter hyper-intensities regions might be considered pre-existing conditions, related to small vessel ischemic disease, especially in older patients.

WT: Segmenting the whole tumor extent (Union of all labels). One should start by loading the T2-FLAIR images and creating a new label for the WT. We recommend to start from the top of

the brain (i.e., superiorly) and since this sub-region is usually the larger with a relatively smooth shape, it is sufficient to make manual delineations every third slice. Then morphological operations of dilation and erosion can be used to fill the in-between axial slices. Finally, smoothing with a Gaussian kernel ($\sigma = 1$) can be used to smooth the jaggedness of the label on coronal and sagittal views.

TC: Segmenting the gross tumor core outline (Union of labels 1, 3, and 4). For this sub-region, it is necessary to check whether there are non-enhancing tumor regions. The TC boundaries can be delineated on every other slice. Then, morphological operations of dilation and erosion can be used to fill the in-between axial slices, followed by a Gaussian smoothing filter to help with the non-continuous delineations on coronal view. Once the TC boundaries are defined, the remaining of the WT will correspond to the ED sub-region ("Label 2"), which is described by hyper-intense signal on the T2-FLAIR volumes.

AT: Segmenting the active and the non-enhancing/necrotic tumor regions. The active tumor (AT - i.e., enhancing rim) is described by areas that show hyper-intensity on T1-Gd when compared to T1, but also when compared to normal/healthy white matter (WM) in T1Gd. Biologically, AT is felt to represent regions where there is leakage of contrast through a disrupted blood-brain barrier that is commonly seen in high grade gliomas. The NET represents non-enhancing tumor regions, as well as transitional/prenecrotic and necrotic regions that belong to the non-enhancing part of the TC, and are typically resected in addition to the AT. The appearance of the NET is typically hypo-intense in T1-Gd when compared to T1, but also when compared to normal/healthy WM in T1-Gd.

To delineate the AT in gliomas, we suggest to use the T1Gd scans and the existing TC outline. One can then set an intensity threshold within this label to distinguish between the high intensity active/enhancing tumor and the low intensity non-enhancing/necrotic (and very tortuous) core regions. Note that the choroid plexus and areas of hemorrhage (when they can be identified by comparing to the native T1 scan), should not be labeled.

LGG: Remarks on low grade gliomas. For low grade gliomas (LGGs), we note that they do not exhibit much contrast enhancement, or ED. Biologically, LGGs may have less blood-brain barrier disruption (leading to less leak of contrast during the scan), and may grow at a rate slow enough to avoid significant edema formation, which results from rapid disruption, irritation, and infiltration of normal brain parenchyma by tumor cells. Specifically, after taking all the above into consideration, in scans of LGGs without an apparent ET area, we consider only the NET and vasogenic ED labels, by observing the texture or the intensity on T2-FLAIR images, whereas in LGG scans without ET and without obvious texture differences across modalities (e.g., small astrocytomas) we consider only the NET label, distinguishing between normal and abnormal brain tissue. The difficulty in estimating the accurate boundaries between tumor and healthy tissue in the operating room is reflected in the segmentation labels as well; there is high uncertainty among neurosurgeons, neuroradiologists, and imaging scientists in delineating these boundaries.

2.3 The BraTS Data Since its Inception

The mpMRI scans made publicly available through the BraTS initiative, describe T1, T1Gd, T2, and T2-FLAIR volumes, acquired with different clinical protocols and various scanners from multiple institutions, mentioned as data contributors in the acknowledgements section. The provided data are distributed after their harmonization, following standardization pre-processing without affecting the apparent information in the images. Specifically, the pre-processing routines applied in all the BraTS mpMRI scans include co-registration to the same anatomical template [6], interpolation to a uniform isotropic resolution ($1mm^3$), and skull-stripping.

2.3.1 Continuously Growing Publicly Available Dataset The BraTS dataset has evolved over the years (2012-2018) with a continuously increasing number of patient cases, as well as through an improvement of the data split used for algorithmic development and evaluation (Table 2).

The first two instances of BraTS (2012-2013) comprised a training and a testing dataset of 35 and 15 mpMRI patient scans, respectively. The results and findings of these two first editions, were summarized in [1], which to date is the most popular and downloaded paper of the IEEE TMI journal since its publication, and reflects the interest of the scientific research community in the BraTS initiative as a publicly available dataset and a community benchmark.

The subsequent three instances of BraTS (2014-2016) received a substantial dataset increase in two waves and also included longitudinal mpMRI scans. The first wave of increase came in during 2014-2015 primarily from contributions of The Cancer Imaging Archive (TCIA) repository [8] and then Heidelberg University, and the second wave of increase happened in 2016 with contributions from the Center for Biomedical Image Computing and Analytics (CBICA) at the University of Pennsylvania (UPenn). In addition, stemming from the analysis of the BraTS 2012-2013 results [1], BraTS 2014-2016 employed ground truth data created by label fusion of top-performing approaches.

In 2017, thanks to additional contributions to the BraTS dataset, from CBICA@UPenn and the University of Alabama in Birmingham (UAB), a validation set was included to facilitate algorithm fine-tuning following a ML paradigm of training, validation, and testing datasets. Notably, in 2017 the number of cases was doubled with respect to the previous year, amounting to 477 cases, which was further increased in 2018 with 542 cases, thanks to contributions from MD Anderson Cancer Center in Texas, the Washington University School of Medicine in St. Louis, and the Tata Memorial Center in India.

2.3.2 Focus Beyond Segmentation BraTS, as indicated by its acronym definition, has primarily focused on the segmentation to brain tumor sub-regions. However, after its first instances (2012-2013), its potential clinical relevance became apparent.

BraTS was introduced with secondary tasks, where the results of the brain tumor segmentation algorithms are used towards promoting further analysis and accelerating discovery. From a clinical perspective these secondary tasks featured in the BraTS challenge can be crucial towards fostering the development of algorithms capable of addressing clinical requirements in a more reliable manner than the current clinical practice. Specifically, to pinpoint the clinical relevance of the segmentation task, in the BraTS instances of 2014-2016, longitudinal scans were included in the publicly available dataset, to evaluate the ability and potential of automated tumor volumetry in assessing disease progression. Along the same lines of research, in the last two instances of BraTS (2017-2018), clinical data of patient age, overall survival, and resection status were included, to facilitate the secondary task of predicting patient overall survival via integrative analyses of radiomic features and ML algorithms.

2.3.3 The Latest BraTS Data The datasets used in BraTS 2017 and 2018 have been updated (since BraTS 2016), with more routine clinically-acquired 3T mpMRI scans and all the ground truth labels have been evaluated, and manually-revised when needed, by expert board-certified neuroradiologists. Ample multi-institutional (n=19) routine clinically-acquired pre-operative mpMRI scans of GBM/HGG and LGG, with pathologically confirmed diagnosis and available OS, were provided as the training, validation and testing data.

The data provided since BraTS 2017 differs significantly from the data provided during the previous BraTS challenges (i.e., 2016 and backwards). Specifically, since BraTS 2017, expert

Table 2: Summarizing the distribution of the BraTS data across the training, validation, and testing sets, since the inception the of BraTS initiative, together with the focused tasks of its BraTS instance.

Year	Total data	Training data	Validation data	Testing data	Tasks	Type of data
2012	50	35	N/A	15	Segmentation	Pre-operative only
2013	60	35	N/A	25	Segmentation	Pre-operative only
2014	238	200	N/A	38	Segmentation Disease progression	Longitudinal
2015	253	200	N/A	53	Segmentation Disease progression	Longitudinal
2016	391	200	N/A	191	Segmentation Disease progression	Longitudinal
2017	477	285	46	146	Segmentation Survival prediction	Pre-operative only
2018	542	285	66	191	Segmentation Survival prediction	Pre-operative only

neuroradiologists have radiologically assessed the complete original TCIA glioma collections (i.e., TCGA-GBM, n=262 [9] and TCGA-LGG, n=199 [10]) and categorized each scan as pre-operative or post-operative. Subsequently, all the pre-operative TCIA scans (i.e., 135 GBM [3] and 108 LGG [4]) were annotated by experts for the various sub-regions and included in the BraTS datasets [2–4].

2.3.4 Data Availability As one of the main objectives of the BraTS initiative is to provide an open source repository for continuous development of algorithms, the data of BraTS 2012-2016 has been made available through the Swiss Medical Image Repository (SMIR - www.smir.ch), and the data of BraTS 2017-2018 through the Image Processing Portal of the CBICA@UPenn (IPP - `ipp.cbica.upenn.edu`). Both platforms feature downloading of datasets, as well as the automatic evaluation of the results submitted by participants.

2.3.5 The Ranking Scheme for the Segmentation Task (BraTS 2017-2018) The ranking scheme followed during the BraTS 2017 and 2018 comprised the ranking of each team relative to its competitors for each of the testing subjects, for each evaluated region (i.e., AT, TC, WT), and for each measure (i.e., Dice and Hausdorff (95%)). For example, in BraTS 2018, each team was ranked for 191 subjects, for 3 regions, and for 2 metrics, which resulted in 1146 individual rankings. The final ranking score was then calculated by averaging across all these individual rankings and then normalized by dividing by the number of teams. This ranking scheme has also been adopted in other challenges with satisfactory results, such as the Ischemic Stroke Lesion Segmentation (ISLES - `http://www.isles-challenge.org/`) challenge [11, 12].

2.3.6 Prediction of Patient Overall Survival (BraTS 2017-2018) We identified 346 GBM patients with overall survival (OS), age, and resection status information. 164 of them had undergone surgery with gross total resection (GTR) status. The distributions of OS of GBM patients across the training, validation and testing datasets were matched (Table 3). The patients were divided in three groups of survival comprising long-survivors (who survived more than 15 months), short-survivors (who survived less than 10 months), and mid-survivors (who survived between 10 and 15 months). These thresholds were derived after statistical consideration of the survival distributions across the

Table 3: The overall survival distribution of patients across the training, validation, and testing sets of BraTS 2017 and 2018.

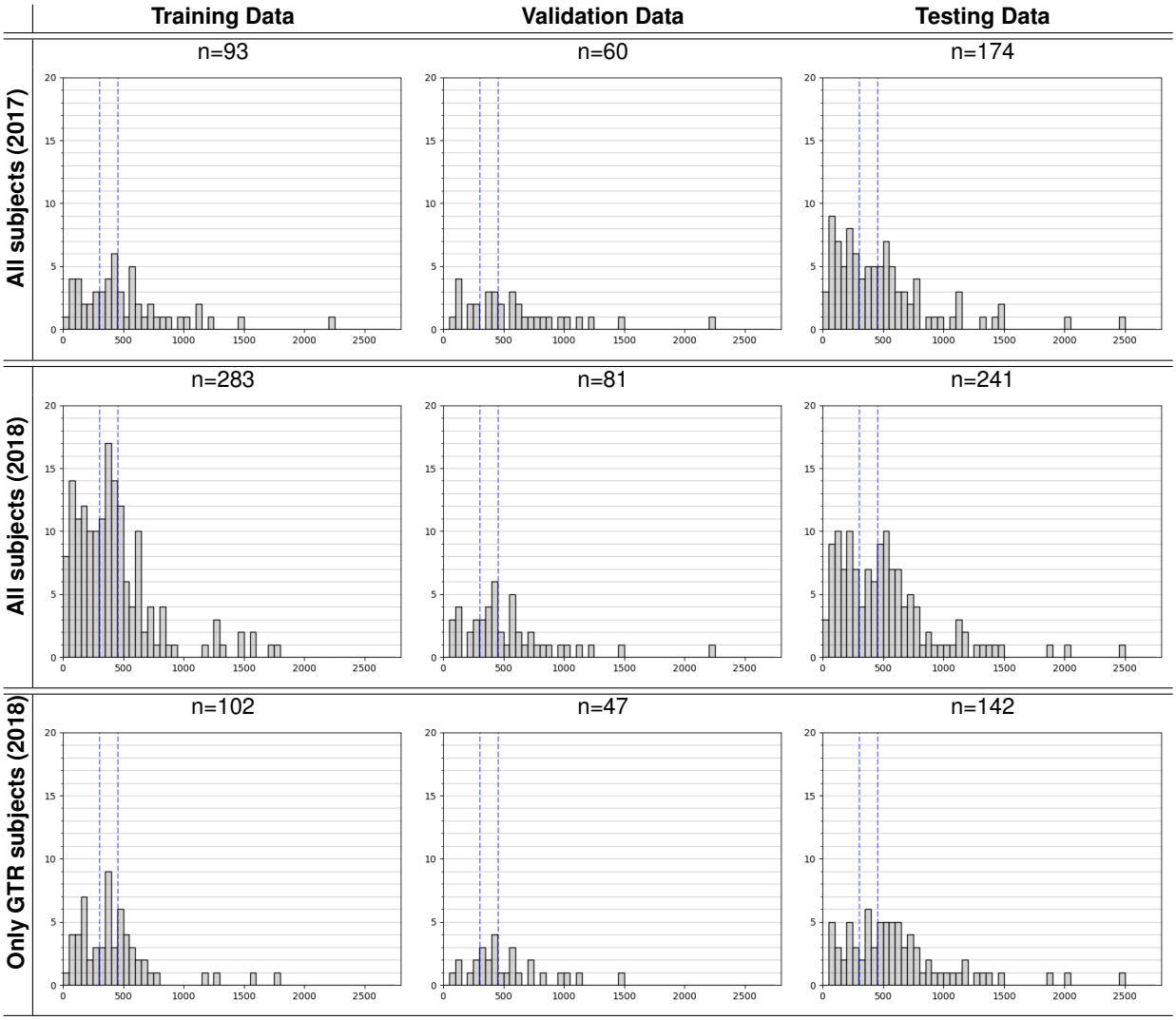

complete dataset. Specifically, we chose these thresholds based on equal quantiles from the median OS (approximately 12.5 months) to avoid potential bias towards one of the survival groups (short- vs long- survivors) and while considering that discrimination of groups should be clinically meaningful. The median OS of the described cohorts is not significantly different from the median OS of GBM patients in several randomized Phase III trials, noting that our cohort consists of unselected patients rather than those eligible for such trials [13, 14].

The population of patients with available OS information was randomly and proportionally divided into the training, validation and testing sets. This process formed a) the training set, consisting of 163 cases (59 with GTR), b) the validation set, consisting of 53 cases (28 with GTR), and c) the testing set, consisting of 130 cases (77 with GTR). Table 3 shows the distribution of patient cases for the task of the OS prediction.

Participating teams were requested to submit OS prediction results in days for each patient with GTR. The evaluation system then automatically classified these into short-, intermediate-, and long-survivors.

2.3.7 Evaluation Framework For consistency purposes both in BraTS 2017 & 2018 challenges, two reference standards were used for the two tasks of the challenge: 1) manual segmentation labels of tumor sub-regions, and 2) clinical data of OS.

The introduction of the validation set since BraTS 2017 allows participants to obtain preliminary results in unseen data, in addition to their cross-validated results on the training data. The ground truth of the validation data was never provided to the participants. Finally, all participants were presented with the same test data, for a limited controlled time-window (48h), before the participants are required to submit their final results for quantitative evaluation and their ranking.

For the segmentation task, and for consistency with the configuration of the previous BraTS challenges, the "Dice score" and the "Hausdorff distance" were used. Expanding upon this evaluation scheme, the metrics of "Sensitivity" and "Specificity" were also used, allowing to determine potential over- or under-segmentations of the tumor sub-regions by participating methods. Since the BraTS 2012-2013 were subsets of the BraTS 2018 test data, performance comparison on the 2012-2013 data will allow for a direct evaluation against the performances reported in [1].

For the task of survival prediction, two evaluation schemes are considered. First, for ranking the participating teams, evaluation will be based on the classification of subjects as long-, intermediate-, and short-survivors. Predictions of the participating teams will be assessed based on classification accuracy (i.e. the number of correctly classified patients) with respect to this grouping. Note that participants are expected to provide predicted survival status only for subjects with resection status of GTR (i.e., Gross Total Resection). In addition, a pairwise error analysis between the predicted and actual survival in days was conducted and the results were shared with the participants, to allow the evaluation of their method for outliers. This analysis was done using the metrics of Mean-Square Error (MSE), median square error (medianSE), standard deviation of the square errors (stdSE), and the spearman correlation coefficient (spearmanR).

3 Results

3.1 BraTS 2012-2013

To emphasize the most interesting results of our previously published analyses summarizing BraTS 2012 and BraTS 2013 [1], we focus into two main points (Fig. 4). First, we note that even though most of the individual automated segmentation methods performed well, they did not outperform the inter-rater agreement, across expert clinicians, who have been trained for years to identify regions of infiltration and distinguish them from healthy brain. Secondly, the fusion of segmentation labels from top-ranked algorithms out-performed all individual methods and was comparable to inter-rater agreement. More specifically, while we observe that individual automated segmentation methods do not necessarily rank equally well in the different tumor segmentation tasks and under all metrics (i.e., when evaluating WT, TC, and AT segmentation, with respect to Dice score and Hausdorff distance), we note that the fused segmentation labels do consistently rank first in all tasks and both metrics. This suggests that ensembles of fused segmentation algorithms may be the favorable approach when translating tumor segmentation methods into clinical practice.

3.2 BraTS 2017 (Testing Phase)

During the testing phase of the BraTS 2017 challenge, we note participation of 48 independent teams [15–62]. Specifically, results for the segmentation task were submitted by 47 teams and for the survival prediction task by 16 teams (1 of which did not participate in the segmentation task).

The ranking of the participating teams depicts a gradual improvement of the ranked approaches (Fig. 5-6). We note that the variability of the ranked approaches (Fig. 5) does not dramatically

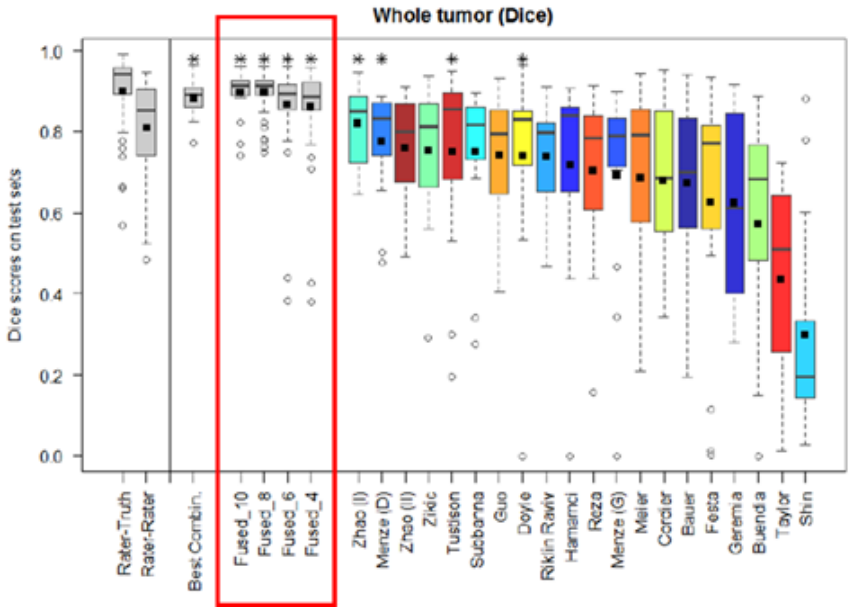

Fig. 4: Summary results of the BraTS 2012-2013. Label fusion (red outline) out-performs all individual methods and the inter-rater agreement. Figure adopted from [1].

Table 4: Top-ranked participating teams in BraTS 2017 for both the segmentation and the survival prediction tasks.

Task	Rank	Team	First Author	Institution	Paper
Segmentation	1	biomedia1	Konstantinos Kamnitsas	Imperial College London, UK	[33]
	2	UCL-TIG	Guotai Wang	University College London (UCL), UK	[55]
	3 (tie)	MIC_DKFZ	Fabian Isensee	Division of Medical Image Computing, German Cancer Research Center (DKFZ), Heidelberg, Germany	[29]
	3 (tie)	CMR	Tsai-Ling Yang	National Taiwan University of Science and Technology, Taipei, Taiwan	[57]
Survival	1	VisionLab	Zeina Shboul	Old Dominion University, USA	[52]
	2	UBERN_UCLM	Alain Jungo	University of Bern, Switzerland	[32]
	3	xfeng	Xue Feng	Biomedical Engineering, University of Virginia, USA	[27]

change across any two sequentially ranked teams, indicating no particular dominance of a method over the other closely ranked methods. In order to assess potential statistically significant performance differences across teams, we also performed a pairwise comparison for significant differences based on 100,000 permutations. This allowed us to include a tie in the 3rd rank of the segmentation task (Table 4). Specifically, the statistical evaluation of the top-ranked teams revealed that the first team was statistically better from the second (p-value¡0.0003), whereas the second team was not statistically better than the third (p¿0.1) and the fourth (p¿0.14), but only from the fifth (p=0.01). This justified the decision of a tie in the third rank.

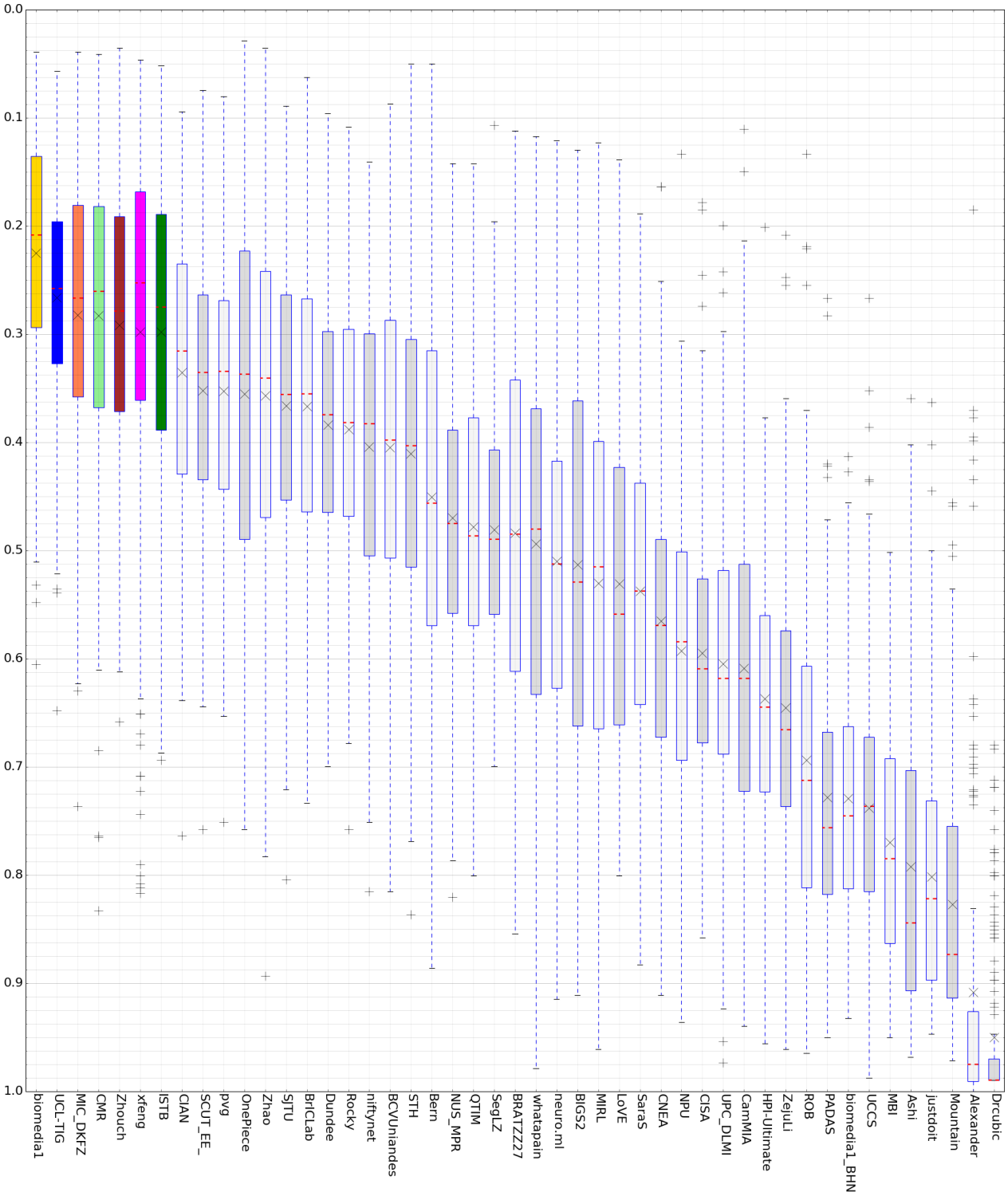

Fig. 5: BraTS 2017 Ranking of all Participating Teams in Segmentation Task. (smaller values are higher ranks)

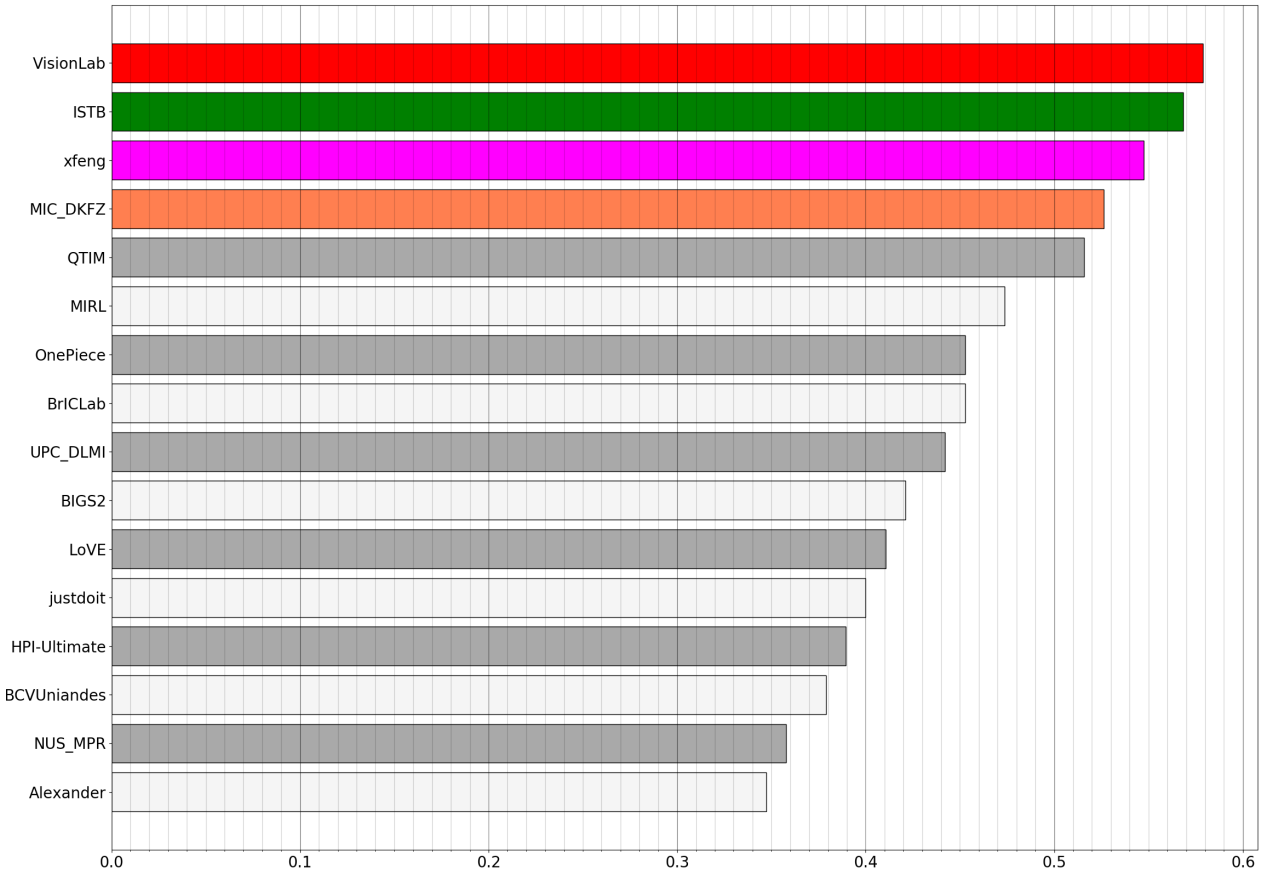

Fig. 6: BraTS 2017 Ranking of all Participating Teams in Survival Task. (larger values are better)

3.3 BraTS 2018 (Testing Phase)

During the testing phase of the BraTS 2018 challenge, we note participation of 63 independent teams [63–125]. Specifically, results for the segmentation task were submitted by 61 teams and for the survival prediction task by 26 teams (2 of which did not participate in the segmentation task).

The BraTS 2018 results for the segmentation of the AT (Suppl.Fig. 9) show a very marked skewness in the distribution of Dice metrics, as seen in the average and median values (crosses and vertical lines on each boxplot). These results illustrate the tendency of most methods to perform relatively well, in terms of median Dice (Median Dice for top 54/63 teams: [0.74-0.85]), but also the difference in levels of robustness as the average Dice is affected by increasing number of outliers in the results (Average Dice of same 54/63 teams: [0.61-0.77]). Segmentation results of the TC (Suppl.Fig. 10) presents a similar pattern, with the results of the AT, across teams. Similarly with observations from previous BraTS instances [1], the top positions are not systematically taken by the same teams, reflecting the added value of fusing segmentation labels from different approaches. In comparison to the AT, segmentation of the TC seems in general to be more robust (i.e., median inter-quantile range (IQR) for Dice of same 54/63 teams, for TC is 0.16, vs. 0.18 for the AT). It is worth mentioning though that the Dice metric is more sensitive to error of the AT, due to its typically much smaller volume. As also noted in previous instances of BraTS, the segmentation of the WT (Suppl.Fig. 11) represents the most robust and accurate segmentation results of the three evaluated tumor compartments (i.e., AT, TC, WT), with a median Dice coefficient of 0.9 for most of the participating teams.

Table 5: Top-ranked participating teams in BraTS 2018 for both the segmentation and the survival prediction tasks.

Task	Rank	Team	First Author	Institution	Paper
Segmentation	1	NVDLMED	Andriy Myronenko	NVIDIA, Santa Clara, USA	[100]
	2	MIC-DKFZ	Fabian Isensee	Division of Medical Image Computing, German Cancer Research Center (DKFZ), Heidelberg, Germany	[86]
	3 (tie)	SCAN	Richard McKinley	Support Centre for Advanced Neuroimaging Inselspital, Bern University Hospital, Switzerland	[97]
	3 (tie)	DL_86_81	Chenhong Zhou	School of Electronic & Information Engineering, South China University of Technology, China	[125]
Survival	1	xfeng	Xue Feng	Biomedical Engineering, University of Virginia, USA	[75]
	2 (tie)	LRDE	Élodie Puybareau	EPITA Research and Development Laboratory, France	[104]
	2 (tie)	SUSTech	Li Sun	Southern University of Science & Technology, China	[111]
	3 (tie)	TRAP	Ujjwal Baid	Shri Guru Gobind Singhji Institute of Engineering and Technology, India	[64]
	3 (tie)	LfB_RWTH	Leon Weninger	Institute of Imaging & Computer Vision, RWTH Aachen University, Germany	[117]

The 95% Hausdorff distance metric is used to characterize the levels of robustness of the automated results. Supplementary Figures 12 through 17 show the Hausdorff metric values for the three evaluated tumor compartments for all teams. Overall, the results for the AT seems to be the most robust for all three tumor labels (median IQR of 1.9 for the same 54/63 teams), followed by the results for the WT and that for the TC (IQR of 4.0 and 5.4 for the same 54/63 teams, respectively).

At the patient-wise ranking of the participating teams (Fig. 7) the distribution follows more closely a gradual improvement of the ranked approaches, similar to results from BraTS 2017. Worth noting is that the variability of the ranking of approaches at the case level does not dramatically change across teams, indicating no particular dominance of a method over the others. We also performed a pairwise comparison for significant differences based on 100,000 permutations that showed the statistically significant performance across teams. Specifically, the statistical evaluation of the top-ranked teams revealed that the first team was statistically better from the second (p-value=0.02), whereas the second team was not statistically better than the third (p=0.06) and the fourth (p=0.07), but only from the fifth (p=0.01). This justified the decision of a tie in the third rank.

Results of the survival task are shown in Fig. 8. Overall, the top-5 approaches obtained an accuracy around 0.6, while the rest of teams obtained an accuracy in the range of [0.15-0.55]. We should clarify that the random choice should be considered the 0.33 since this is a 3-class classification.

The final top-performing participating teams positioned in ranks 1-3 are shown in Table 5.

4 Discussion

4.1 Performance of Automated Segmentation Methods

While the accuracy of individual automated segmentation methods has improved, we note that their level of robustness is still inferior to expert performance, i.e., inter-rater agreement. This robustness

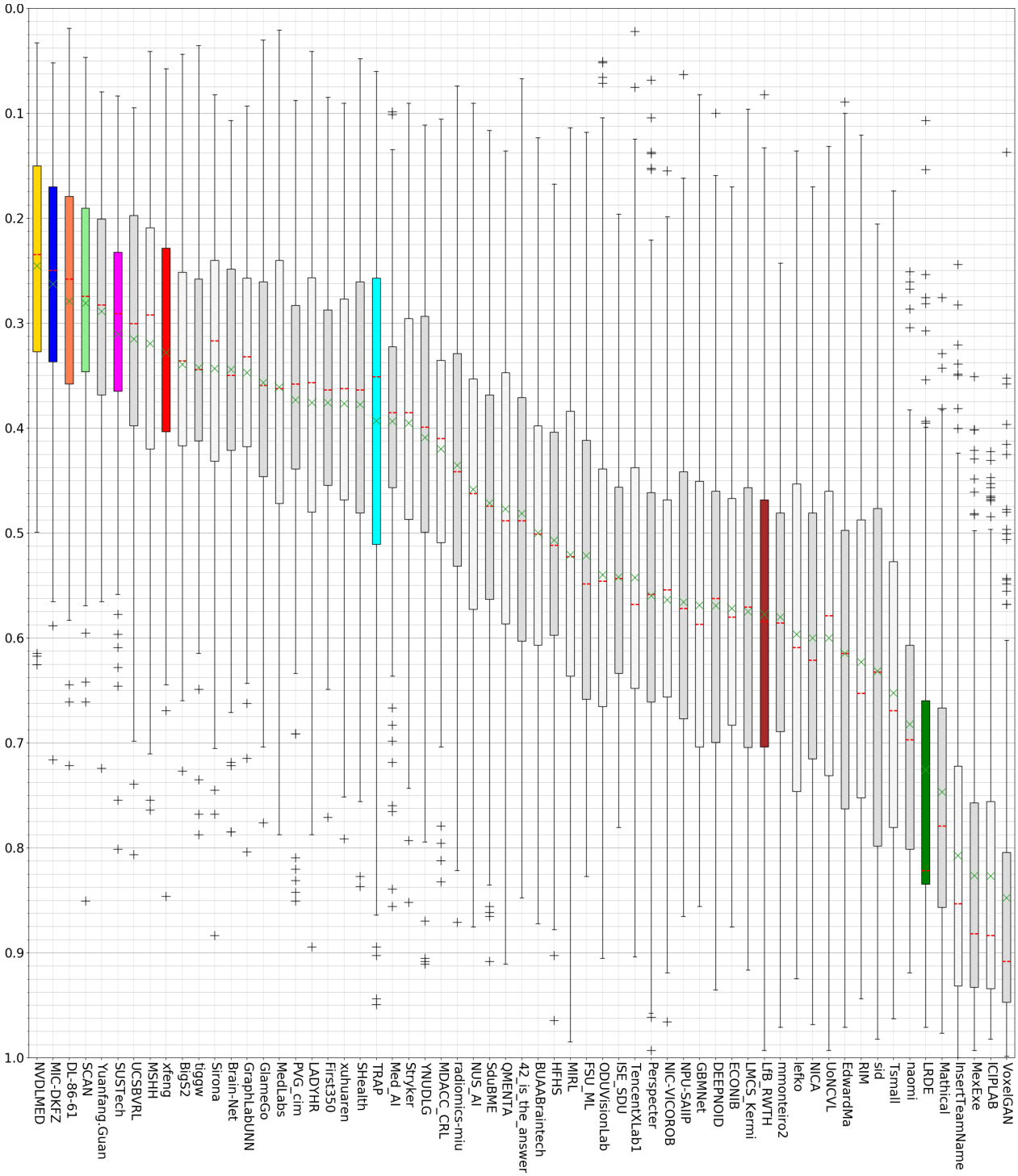

Fig. 7: BraTS 2018 Ranking of all Participating Teams in Segmentation Task. (smaller values are higher ranks)

is expected to be continuously improving as the training set increases in size, in virtue of capturing and describing more diverse patient populations, along with improved training schemes and ML architectures. Beyond these speculative expectations, the results of our quantitative analyses

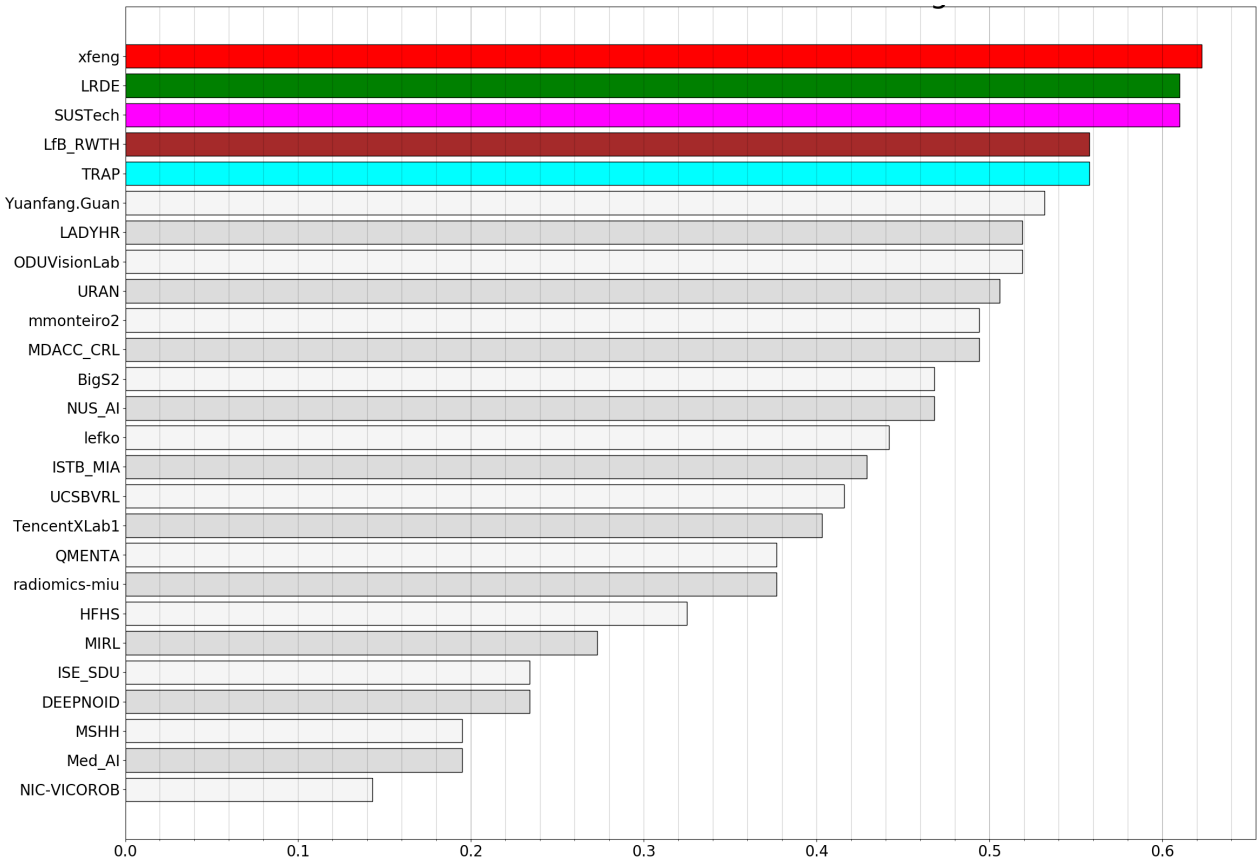

Fig. 8: BraTS 2018 Ranking of all Participating Teams in Survival Task. (larger values are better)

support that the fusion of segmentation labels from various individual automated methods shows robustness superior to the ground truth inter-rater agreement (provided by clinical experts), in terms of both accuracy and consistency across subjects. However, proposed strategies to ensemble several models correspond to one practical way to reduce outliers and improve the precision of automated segmentation systems, by means of consensus segmentation across different models. We consider future research essential, in order to improve the robustness of individual approaches by increasing the ability of segmentation systems to handle confounding effects typically seen in images acquired using routine clinical workflows. Related to BraTS such effects include, but are not limited to, a) the presence of blood products, b) ”air-pockets”/resection cavities in post-operative scans, c) better differentiation (or handling) of non-GBM entities, and d) improved performance for low-grade gliomas, featuring diffuse boundaries, especially while considering cases without AT sub-regions, and e) high sensitivity to effectively detect and assess their slow progression.

4.2 BraTS Ranking Schema

The BraTS challenge recently adopted a case-wise ranking schema, which enables a more clinically-relevant evaluation of participating teams, as it considers the complexity of patient cases that can vary significantly. Furthermore, the additional featured evaluation of statistical significance of differences across algorithmic results, also enables the evaluation of results across different instances of the BraTS challenge, which in turns enables a thorough analysis of the improvement attained over the last seven years of the BraTS initiative.

4.3 Beyond Segmentation

Importantly, two more clinically-relevant tasks/sub-challenges have been complementarily added in the BraTS initiative during these past seven years, aiming at emphasizing the clinical relevance of the brain tumor segmentation task. Both these clinically-relevant tasks promote the natural utilization of segmentation labels to answer clinical questions, address clinical requirements, and potentially support the clinical decision-making process. The ultimate goal of these additions was to evaluate the potential usability and pave the way of automated segmentation methods towards their translation to routine clinical practice.

4.3.1 Assessment of Disease Progression The inclusion of longitudinal (i.e., follow up) mpMRI scans took place during the BraTS 2014-2016 instances. In clinical practice, assessment of disease progression is to date performed through the Response Evaluation Criteria In Solid Tumours (RECIST) [126–129] and the Response Assessment in Neuro-Oncology (RANO) criteria [130], whose quantitative component is based on the relative change of tumor size (i.e., percentile changes) measured by the longest two axes of the assessed tumor. In this regard, we postulate that automated algorithms performing brain tumor volumetric segmentation (i.e., in three dimensions) should yield reliable comparable (if not better) estimates of volumetric tumor changes.

4.3.2 Prediction of Overall Survival The inclusion of the OS prediction task took place during the BraTS 2017-2018 instances and has highlighted (or rather confirmed) the difficulties of Deep Learning (DL) approaches to handle small training sets, and the superiority of traditional ML approaches. While this finding clearly calls for larger training sets, it also identifies the need for potential synergies between DL and traditional ML approaches as we transition to larger training sets in the future, which can include more non-uniformly distributed clinical and/or molecular information. In other words, there is a need to develop advanced ML approaches able to handle the large existing heterogeneity of the patient-specific information available in the clinics, e.g., radiogenomics [131–138], RIS reports.

4.4 Future Directions for the BraTS Initiative

The current trend over the years of the previous BraTS instances highlights (or rather confirms) a) the superiority of DL over traditional ML approaches in the segmentation task (and particularly in terms of Dice), and, in contrast, b) the struggle of DL and the superiority of traditional ML approaches, assessing more clinically-relevant problems, such as the prediction of clinical outcome (i.e., overall survival), where smaller training sets are typically available and need to be handled.

Concentrating on the segmentation task, in terms of algorithmic design, the current general consensus seems to point in the direction of tackling the problem in a hierarchical/cascaded way, by first distinguishing between normal and abnormal/tumorous tissue, and then proceeding with the segmentation of the tumor sub-regions. Alternative research directions include the enhancement of the flexibility of DL systems that might lack a given set of input images [139], as a transition measure towards worldwide adoption of the standardization initiatives for GBM imaging [140].

There are many clinical endpoints where the BraTS initiative can have a potential impact and these include, but not limited to: a) training systems for neuroradiology trainees, b) differential diagnosis (e.g., metastases differentiation, disease progression assessment, radio-phenotyping), c) prognosis (e.g., prediction of overall survival, drug-response prediction), d) radiation therapy planning. However, for any of these to be potentially considered wider application of the developed methods needs to take place, which is why we created the BraTS algorithmic repository, and a

closer collaboration with the clinical expertise is fundamental to tailor the design of the BraTS challenges towards an effective exploitation and translation of research findings into clinical practice.

5 Acknowledgements

Importantly, we would like to express our gratitude to all the data contributing institutions that assisted in putting together the publicly-available multi-institutional mpMRI BraTS dataset, acquired with different clinical protocols and various scanners. Note that without these contributions the BraTS initiative would have never been feasible. These data contributors are: 1) Center for Biomedical Image Computing and Analytics (CBICA), University of Pennsylvania (UPenn), PA, USA, 2) University of Alabama at Birmingham, AL, USA, 3) Heidelberg University, Germany, 4) University Hospital of Bern, Switzerland, 5) University of Debrecen, Hungary, 6) Henry Ford Hospital, MI, USA, 7) University of California, CA, USA, 8) MD Anderson Cancer Center, TX, USA, 9) Emory University, GA, USA, 10) Mayo Clinic, MN, USA, 11) Thomas Jefferson University, PA, USA, 12) Duke University School of Medicine, NC, USA, 13) Saint Joseph Hospital and Medical Center, AZ, USA, 14) Case Western Reserve University, OH, USA, 15) University of North Carolina, NC, USA, 16) Fondazione IRCCS Instituto Neuroligico C. Besta, Italy, 17) MD Anderson Cancer Center, TX, USA, 18) Washington University School of Medicine in St. Louis, MO, USA, and 19) Tata Memorial Center, Mumbai, India. Note that data from institutions 6-16 are provided through The Cancer Imaging Archive (TCIA - http://www.cancerimagingarchive.net/), supported by the Cancer Imaging Program (CIP) of the National Cancer Institute (NCI) of the National Institutes of Health (NIH).

We would also like to thank the sponsorship offered by the CBICA@UPenn for the plaques provided to the top-ranked participating teams of the challenge each year, as well as Intel AI for sponsoring the monetary prizes of total value of $5,000, awarded to the three top-ranked participating teams of the BraTS 2018 challenge, who also shared publicly their containerized algorithm in the BraTS algorithmic repository: `github.com/BraTS/Instructions/blob/master/Repository_Links.md` & `hub.docker.com/u/brats/`.

This work was supported in part by the 1) National Institute of Neurological Disorders and Stroke (NINDS) of the NIH R01 grant with award number R01-NS042645, 2) Informatics Technology for Cancer Research (ITCR) program of the NCI/NIH U24 grant with award number U24-CA189523, 3) Swiss Cancer League, under award number KFS-3979-08-2016, 4) Swiss National Science Foundation, under award number 169607. The content of this publication is solely the responsibility of the authors and does not necessarily represent the official views of NIH or any of the other funding bodies.

References

1. Menze, B.H., Jakab, A., Bauer, S., Kalpathy-Cramer, J., Farahani, K., Kirby, J., et al.: The multimodal brain tumor image segmentation benchmark (brats). IEEE Transactions on Medical Imaging **34** (2015) 1993–2024
2. Bakas, S., Akbari, H., Sotiras, A., Bilello, M., Rozycki, M., Kirby, J.S., et al.: Advancing the cancer genome atlas glioma mri collections with expert segmentation labels and radiomic features. Nature Scientific Data **4** (2017) 170117
3. Bakas, S., Akbari, H., Sotiras, A., Bilello, M., Rozycki, M., Kirby, J.S., et al.: Segmentation labels and radiomic features for the pre-operative scans of the tcga-gbm collection. T. C. I. Archive (2017)
4. Bakas, S., Akbari, H., Sotiras, A., Bilello, M., Rozycki, M., Kirby, J.S., et al.: Segmentation labels and radiomic features for the pre-operative scans of the tcga-lgg collection. T. C. I. Archive (2015)
5. Zwanenburg, A., Leger, S., Vallires, M., Lck, S., I.B.S.I: Image biomarker standardisation initiative. arXiv preprint arXiv:1612.07003 (2016)
6. Rohlfing, T., Zahr, N.M., Sullivan, E.V., Pfefferbaum, A.: The sri24 multi-channel atlas of normal adult human brain structure. Human brain mapping **31** (2010) 798–819

7. Haller, S., Kovari, E., Herrmann, F.R., Cuvinciuc, V., Tomm, A.M., Zulian, G.B., Lovblad, K.O., Giannakopoulos, P., Bouras, C.: Do brain t2/flair white matter hyperintensities correspond to myelin loss in normal aging. a radiologic-neuropathologic correlation study. Acta Neuropathol Commun **1**(14) (2013) 1–7
8. Clark, K., Vendt, B., Smith, K., Freymann, J., Kirby, J., Koppel, P., et al.: The cancer imaging archive (tcia): Maintaining and operating a public information repository. Journal of Digital Imaging **26** (2013) 1045–1057
9. Scarpace, L., Mikkelsen, T., Cha, S., Rao, S., Tekchandani, S., Gutman, D., et al.: Radiology data from the cancer genome atlas glioblastoma multiforme [tcga-gbm] collection. The Cancer Imaging Archive (2016)
10. Pedano, N., Flanders, A.E., Scarpace, L., Mikkelsen, T., Eschbacher, J.M., Hermes, B., et al.: Radiology data from the cancer genome atlas low grade glioma [tcga-lgg] collection. The Cancer Imaging Archive (2016)
11. Maier, O., Menze, B.H., von der Gablentz, J., Hni, L., Heinrich, M.P., Liebrand, M., et al.: Isles 2015 - a public evaluation benchmark for ischemic stroke lesion segmentation from multispectral mri. Medical Image Analysis **35** (2017) 250–269
12. Winzeck, S., Hakim, A., McKinley, R., Pinto, J., Alves, V., Silva, C., et al.: Isles 2016 and 2017-benchmarking ischemic stroke lesion outcome prediction based on multispectral mri. Frontiers in neurology **9** (2018) 679–679
13. Stupp, R., Hegi, M.E., Mason, W.P., van den Bent, M.J., Taphoorn, M.J.B., Janzer, R.C., et al.: Effects of radiotherapy with concomitant and adjuvant temozolomide versus radiotherapy alone on survival in glioblastoma in a randomised phase iii study: 5-year analysis of the eortc-ncic trial. The Lancet Oncology **10** (2009) 459–466
14. Gilbert, M.R., Wang, M., Aldape, K.D., Stupp, R., Hegi, M.E., Jaeckle, K.A., et al.: Dose-dense temozolomide for newly diagnosed glioblastoma: A randomized phase iii clinical trial. Journal of Clinical Oncology **31** (2013) 4085–4091
15. Alex, V., Safwan, M., Krishnamurthi, G.: Automatic segmentation and overall survival prediction in gliomas using fully convolutional neural network and texture analysis. BrainLes 2017, Springer LNCS **10670** (2018) 216–225
16. Amorim, P.H.A., Chagas, V.S., Escudero, G., Oliveira, D.D.C., Pereira, S.M., Santos, H.M., Scussel, A.A.: 3d u-nets for brain tumor segmentation in miccai 2017 brats challenge. MICCAI BraTS 2017 Pre-proceedings - https://www.cbica.upenn.edu/sbia/Spyridon.Bakas/MICCAI_BraTS/MICCAI_BraTS_2017_proceedings_shortPapers.pdf (2017) 9–14
17. Andermatt, S., Pezold, S., Cattin, P.: Multi-dimensional gated recurrent units for brain tumor segmentation. MICCAI BraTS 2017 Pre-proceedings - https://www.cbica.upenn.edu/sbia/Spyridon.Bakas/MICCAI_BraTS/MICCAI_BraTS_2017_proceedings_shortPapers.pdf (2017) 15–19
18. Beers, A., Chang, K., Brown, J., Sartor, E., Mammen, C., Gerstner, E., Rosen, B., Kalpathy-Cramer, J.: Sequential 3d u-nets for brain tumor segmentation. MICCAI BraTS 2017 Pre-proceedings - https://www.cbica.upenn.edu/sbia/Spyridon.Bakas/MICCAI_BraTS/MICCAI_BraTS_2017_proceedings_shortPapers.pdf (2017) 20–23
19. Bharath, H.N., Colleman, S., Sima, D., Huffel, S.V.: Tumor segmentation from multimodal mri using random forest with superpixel and tensor based feature extraction. BrainLes 2017, Springer LNCS **10670** (2018) 463–473
20. Cao, S., Qian, B., Yin, C., Li, X., Chang, S.: 3d u-net for multimodal brain tumor segmentation. MICCAI BraTS 2017 Pre-proceedings - https://www.cbica.upenn.edu/sbia/Spyridon.Bakas/MICCAI_BraTS/MICCAI_BraTS_2017_proceedings_shortPapers.pdf (2017) 30–33
21. Casamitjana, A., Catá, M., Sánchez, I., Combalia, M., Vilaplana, V.: Cascaded v-net using roi masks for brain tumor segmentation. BrainLes 2017, Springer LNCS **10670** (2018) 381–391
22. Castillo, L.S., Daza, L.A., Rivera, L.C., Arbeláez, P.: Brain tumor segmentation and parsing on mris using multiresolution neural networks. BrainLes 2017, Springer LNCS **10670** (2018) 332–343
23. Chen, S., Ding, C., Zhou, C.: Brain tumor segmentation with label distribution learning and multi-level feature representation. MICCAI BraTS 2017 Pre-proceedings - https://www.cbica.upenn.edu/sbia/Spyridon.Bakas/MICCAI_BraTS/MICCAI_BraTS_2017_proceedings_shortPapers.pdf (2017) 50–53
24. Colmeiro, R.G.R., Verrastro, C.A., Grosges, T.: Multimodal brain tumor segmentation using 3d convolutional networks. BrainLes 2017, Springer LNCS **10670** (2018) 226–240
25. Dong, S.: A separate 3d-segnet architecture for brain tumor segmentation. MICCAI BraTS 2017 Pre-proceedings - https://www.cbica.upenn.edu/sbia/Spyridon.Bakas/MICCAI_BraTS/MICCAI_BraTS_2017_proceedings_shortPapers.pdf (2017) 54–60
26. Eaton-Rosen, Z., Li, W., Wang, G., Vercauteren, T., Bisdas, S., Ourselin, S., Cardoso, M.J.: Using niftynet to ensemble convolutional neural nets for the brats challenge. MICCAI BraTS 2017 Pre-proceedings - https://www.cbica.upenn.edu/sbia/Spyridon.Bakas/MICCAI_BraTS/MICCAI_BraTS_2017_proceedings_shortPapers.pdf (2017) 61–66
27. Feng, X., Meyer, C.: Patch-based 3d u-net for brain tumor segmentation. MICCAI BraTS 2017 Pre-proceedings - https://www.cbica.upenn.edu/sbia/Spyridon.Bakas/MICCAI_BraTS/MICCAI_BraTS_2017_proceedings_shortPapers.pdf (2017) 67–72
28. Hu, Y., Xia, Y.: 3d deep neural network-based brain tumor segmentation using multimodality magnetic resonance sequences. BrainLes 2017, Springer LNCS **10670** (2018) 423–434

29. Isensee, F., Kickingereder, P., Wick, W., Bendszus, M., Maier-Hein, K.H.: Brain tumor segmentation and radiomics survival prediction: Contribution to the brats 2017 challenge. BrainLes 2017, Springer LNCS **10670** (2018) 287–297
30. Islam, M., Ren, H.: Multi-modal pixelnet for brain tumor segmentation. BrainLes 2017, Springer LNCS **10670** (2018) 298–308
31. Jesson, A., Arbel, T.: Brain tumor segmentation using a 3d fcn with multi-scale loss. BrainLes 2017, Springer LNCS **10670** (2018) 392–402
32. Jungo, A., McKinley, R., Meier, R., Knecht, U., Vera, L., Pérez-Beteta, J., Molina-García, D., Pérez-García, V.M., Wiest, R., Reyes, M.: Towards uncertainty-assisted brain tumor segmentation and survival prediction. BrainLes 2017, Springer LNCS **10670** (2018) 474–485
33. Kamnitsas, K., Bai, W., Ferrante, E., McDonagh, S., Sinclair, M., Pawlowski, N., Rajchl, M., Lee, M., Kainz, B., Rueckert, D., Glocker, B.: Ensembles of multiple models and architectures for robust brain tumour segmentation. BrainLes 2017, Springer LNCS **10670** (2018) 450–462
34. Karnawat, A., Prasanna, P., Madabushi, A., Tiwari, P.: Radiomics-based convolutional neural network (radcnn) for brain tumor segmentation on multi-parametric mri. MICCAI BraTS 2017 Pre-proceedings - https://www.cbica.upenn.edu/sbia/Spyridon.Bakas/MICCAI_BraTS/MICCAI_BraTS_2017_proceedings_shortPapers.pdf (2017) 147–153
35. Kim, G.: Brain tumor segmentation using deep fully convolutional neural networks. BrainLes 2017, Springer LNCS **10670** (2018) 344–357
36. Krivov, E., Pisov, M., Belyaev, M.: Mri augmentation via elastic registration for brain lesions segmentation. BrainLes 2017, Springer LNCS **10670** (2018) 369–380
37. Li, Y., Shen, L.: Deep learning based multimodal brain tumor diagnosis. BrainLes 2017, Springer LNCS **10670** (2018) 149–158
38. Li, Z., Wang, Y., Yu, J.: Brain tumor segmentation using an adversarial network. MICCAI BraTS 2017 Pre-proceedings - https://www.cbica.upenn.edu/sbia/Spyridon.Bakas/MICCAI_BraTS/MICCAI_BraTS_2017_proceedings_shortPapers.pdf (2017) 164–168
39. Li, X., Zhang, X., Luo, Z.: Brain tumor segmentation via 3d fully dilated convolutional networks. MICCAI BraTS 2017 Pre-proceedings - https://www.cbica.upenn.edu/sbia/Spyridon.Bakas/MICCAI_BraTS/MICCAI_BraTS_2017_proceedings_shortPapers.pdf (2017) 175–179
40. Liu, L., Nie, D., Wang, Q., Shen, D.: A location sensitive brain tumor segmentation method. MICCAI BraTS 2017 Pre-proceedings - https://www.cbica.upenn.edu/sbia/Spyridon.Bakas/MICCAI_BraTS/MICCAI_BraTS_2017_proceedings_shortPapers.pdf (2017) 180–187
41. Lopez, M.M., Ventura, J.: Dilated convolutions for brain tumor segmentation in mri scans. BrainLes 2017, Springer LNCS **10670** (2018) 253–262
42. Mang, A., Tharakan, S., Gholami, A., Himthani, N., Subramanian, S., Levitt, J., Azmat, M., Scheufele, K., Mehl, M., Davatzikos, C., Barth, B., Biros, G.: Sibia-gls: Scalable biophysics-based image analysis for glioma segmentation. MICCAI BraTS 2017 Pre-proceedings - https://www.cbica.upenn.edu/sbia/Spyridon.Bakas/MICCAI_BraTS/MICCAI_BraTS_2017_proceedings_shortPapers.pdf (2017) 197–204
43. McKinley, R., Jungo, A., Wiest, R., Reyes, M.: Pooling-free fully convolutional networks with dense skip connections for semantic segmentation, with application to brain tumor segmentation. BrainLes 2017, Springer LNCS **10670** (2018) 169–177
44. Osman, A.F.I.: Automated brain tumor segmentation on magnetic resonance images and patients overall survival prediction using support vector machines. BrainLes 2017, Springer LNCS **10670** (2018) 435–449
45. Pawar, K., Chen, Z., Shah, N.J., Egan, G.: Residual encoder and convolutional decoder neural network for glioma segmentation. BrainLes 2017, Springer LNCS **10670** (2018) 263–273
46. Phophalia, A., Maji, P.: Multimodal brain tumor segmentation using ensemble of forest method. BrainLes 2017, Springer LNCS **10670** (2018) 159–168
47. Pourreza, R., Zhuge, Y., Ning, H., Miller, R.: Brain tumor segmentation in mri scans using deeply-supervised neural networks. BrainLes 2017, Springer LNCS **10670** (2018) 320–331
48. Revanuru, K., Shah, N.: Fully automatic brain tumour segmentation using random forests and patient survival prediction using xgboost. MICCAI BraTS 2017 Pre-proceedings - https://www.cbica.upenn.edu/sbia/Spyridon.Bakas/MICCAI_BraTS/MICCAI_BraTS_2017_proceedings_shortPapers.pdf (2017) 239–243
49. Rezaei, M., Harmuth, K., Gierke, W., Kellermeier, T., Fischer, M., Yang, H., Meinel, C.: A conditional adversarial network for semantic segmentation of brain tumor. BrainLes 2017, Springer LNCS **10670** (2018) 241–252
50. Sedlar, S.: Brain tumor segmentation using a multi-path cnn based method. BrainLes 2017, Springer LNCS **10670** (2018) 403–422
51. Shaikh, M., Anand, G., Acharya, G., Amrutkar, A., Alex, V., Krishnamurthi, G.: Brain tumor segmentation using dense fully convolutional neural network. BrainLes 2017, Springer LNCS **10670** (2018) 309–319
52. Shboul, Z.A., Vidyaratne, L., Alam, M., Iftekharuddin, K.M.: Glioblastoma and survival prediction. BrainLes 2017, Springer LNCS **10670** (2018) 358–368

53. Shen, H., Wang, R., Zhang, J., McKenna, S.: Symmetry-driven fully convolutional network for brain tumor segmentation. MICCAI BraTS 2017 Pre-proceedings - https://www.cbica.upenn.edu/sbia/Spyridon.Bakas/MICCAI_BraTS/MICCAI_BraTS_2017_proceedings_shortPapers.pdf (2017) 274–278
54. Soltaninejad, M., Zhang, L., Lambrou, T., Yang, G., Allinson, N., Ye, X.: Mri brain tumor segmentation and patient survival prediction using random forests and fully convolutional networks. BrainLes 2017, Springer LNCS **10670** (2018) 204–215
55. Wang, G., Li, W., Ourselin, S., Vercauteren, T.: Automatic brain tumor segmentation using cascaded anisotropic convolutional neural networks. BrainLes 2017, Springer LNCS **10670** (2018) 178–190
56. Wang, C., Smedby, O.: Automatic brain tumor segmentation using 2.5d u-nets. MICCAI BraTS 2017 Pre-proceedings - https://www.cbica.upenn.edu/sbia/Spyridon.Bakas/MICCAI_BraTS/MICCAI_BraTS_2017_proceedings_shortPapers.pdf (2017) 292–296
57. Yang, T.L., Ou, Y.N., Huang, T.Y.: Automatic segmentation of brain tumor from mr images using segnet: selection of training data sets. MICCAI BraTS 2017 Pre-proceedings - https://www.cbica.upenn.edu/sbia/Spyridon.Bakas/MICCAI_BraTS/MICCAI_BraTS_2017_proceedings_shortPapers.pdf (2017) 309–312
58. Zhao, X., Wu, Y., Song, G., Li, Z., Zhang, Y., Fan, Y.: 3d brain tumor segmentation through integrating multiple 2d fcnns. BrainLes 2017, Springer LNCS **10670** (2018) 191–203
59. Zhao, L.: Automatic brain tumor segmentation with 3d deconvolution network with dilated inception block. MICCAI BraTS 2017 Pre-proceedings - https://www.cbica.upenn.edu/sbia/Spyridon.Bakas/MICCAI_BraTS/MICCAI_BraTS_2017_proceedings_shortPapers.pdf (2017) 316–320
60. Zhou, F., Li, T., Li, H., Zhu, H.: Tpcnn: Two-phase patch-based convolutional neural network for automatic brain tumor segmentation and survival prediction. BrainLes 2017, Springer LNCS **10670** (2018) 274–286
61. Zhou, C., Ding, C., Lu, Z., Zhang, T.: Brain tumor segmentation with cascaded convolutional neural networks. MICCAI BraTS 2017 Pre-proceedings - https://www.cbica.upenn.edu/sbia/Spyridon.Bakas/MICCAI_BraTS/MICCAI_BraTS_2017_proceedings_shortPapers.pdf (2017) 328–333
62. Zhu, J., Wang, D., Teng, Z., Lió, P.: A multi-pathway 3d dilated convolutional neural network for brain tumor segmentation. MICCAI BraTS 2017 Pre-proceedings - https://www.cbica.upenn.edu/sbia/Spyridon.Bakas/MICCAI_BraTS/MICCAI_BraTS_2017_proceedings_shortPapers.pdf (2017) 342–347
63. Albiol, A., Albiol, A., Albiol, F.: Extending 2d deep learning architectures to 3d image segmentation problems. BrainLes 2018, Springer LNCS **11384** (2019) 73–82
64. Baid, U., Talbar, S., Rane, S., Gupta, S., Thakur, M.H., Moiyadi, A., Thakur, S., Mahajan, A.: Deep learning radiomics algorithm for gliomas (drag) model: A novel approach using 3d unet based deep convolutional neural network for predicting survival in gliomas. BrainLes 2018, Springer LNCS **11384** (2019) 369–379
65. Banerjee, S., Mitra, S., Shankar, B.U.: Multi-planar spatial-convnet for segmentation and survival prediction in brain cancer. BrainLes 2018, Springer LNCS **11384** (2019) 94–104
66. Benson, E., Pound, M.P., French, A.P., Jackson, A.S., Pridmore, T.P.: Deep hourglass for brain tumor segmentation. BrainLes 2018, Springer LNCS **11384** (2019) 419–428
67. Cabezas, M., Valverde, S., González-Villá, S., Cérigues, A., Salem, M., Kushibar, K., Bernal, J., Oliver, A., Salvi, J., Lladó, X.: Survival prediction using ensemble tumor segmentation and transfer learning. MICCAI BraTS 2018 Pre-proceedings - https://www.cbica.upenn.edu/sbia/Spyridon.Bakas/MICCAI_BraTS/MICCAI_BraTS_2018_proceedings_shortPapers.pdf (2018) 54–62
68. Carver, E., Liu, C., Zong, W., Dai, Z., Snyder, J.M., Lee, J., Wen, N.: Automatic brain tumor segmentation and overall survival prediction using machine learning algorithms. BrainLes 2018, Springer LNCS **11384** (2019) 406–418
69. Chandra, S., Vakalopoulou, M., Fidon, L., Battistella, E., Estienne, T., Sun, R., Robert, C., Deutsch, E., Paragios, N.: Context aware 3d cnns for brain tumor segmentation. BrainLes 2018, Springer LNCS **11384** (2019) 299–310
70. Chang, Y.J., Lin, Z.S., Yang, T.L., Huang, T.Y.: Automatic segmentation of brain tumor from 3d mr images using a 2d convolutional neural network. MICCAI BraTS 2018 Pre-proceedings - https://www.cbica.upenn.edu/sbia/Spyridon.Bakas/MICCAI_BraTS/MICCAI_BraTS_2018_proceedings_shortPapers.pdf (2018) 83–90
71. Chen, W., Liu, B., Peng, S., Sun, J., Qiao, X.: S3d-unet: Separable 3d u-net for brain tumor segmentation. BrainLes 2018, Springer LNCS **11384** (2019) 358–368
72. Choudhury, A.R., Vanguri, R., Jambawalikar, S.R., Kumar, P.: Segmentation of brain tumors using deeplabv3+. BrainLes 2018, Springer LNCS **11384** (2019) 154–167
73. Dai, L., Li, T., Shu, H., Zhong, L., Shen, H., Zhu, H.: Automatic brain tumor segmentation with domain adaptation. BrainLes 2018, Springer LNCS **11384** (2019) 380–392
74. Fang, L., He, H.: Three pathways u-net for brain tumor segmentation. MICCAI BraTS 2018 Pre-proceedings - https://www.cbica.upenn.edu/sbia/Spyridon.Bakas/MICCAI_BraTS/MICCAI_BraTS_2018_proceedings_shortPapers.pdf (2018) 119–126
75. Feng, X., Tustison, N., Meyer, C.: Brain tumor segmentation using an ensemble of 3d u-nets and overall survival prediction using radiomic features. BrainLes 2018, Springer LNCS **11384** (2019) 279–288

76. Fridman, N.: Brain tumor detection and segmentation using deep learning u-net on multi modal mri. MICCAI BraTS 2018 Pre-proceedings - https://www.cbica.upenn.edu/sbia/Spyridon.Bakas/MICCAI_BraTS/MICCAI_BraTS_2018_proceedings_shortPapers.pdf (2018) 135–143
77. Gates, E., Pauloski, J.G., Schellingerhout, D., Fuentes, D.: Glioma segmentation and a simple accurate model for overall survival prediction. BrainLes 2018, Springer LNCS **11384** (2019) 476–484
78. Gering, D., Sun, K., Avery, A., Chylla, R., Vivekanandan, A., Kohli, L., Knapp, H., Paschke, B., Young-Moxon, B., King, N., Mackie, T.: Semi-automatic brain tumor segmentation by drawing long axes on multi-plane reformat. BrainLes 2018, Springer LNCS **11384** (2019) 441–455
79. Gholami, A., Subramanian, S., Shenoy, V., Himthani, N., Yue, X., Zhao, S., Jin, P., Biros, G., Keutzer, K.: A novel domain adaptation framework for medical image segmentation. BrainLes 2018, Springer LNCS **11384** (2019) 289–298
80. Han, W.S., Han, I.S.: Neuromorphic neural network for multimodal brain image segmentation and overall survival analysis. BrainLes 2018, Springer LNCS **11384** (2019) 178–188
81. Hu, X., Huang, W., Kong, D., Guo, S., Scott, M.R.: Brainnet: 3d local refinement network for brain tumor segmentation. MICCAI BraTS 2018 Pre-proceedings - https://www.cbica.upenn.edu/sbia/Spyridon.Bakas/MICCAI_BraTS/MICCAI_BraTS_2018_proceedings_shortPapers.pdf (2018) 179–187
82. Hu, X., Li, H., Zhao, Y., Dong, C., Menze, B.H., Piraud, M.: Hierarchical multi-class segmentation of glioma images using networks with multi-level activation function. BrainLes 2018, Springer LNCS **11384** (2019) 116–127
83. Hu, Y., Liu, X., Wen, X., Niu, C., Xia, Y.: Brain tumor segmentation on multimodal mr imaging using multi-level upsampling in decoder. BrainLes 2018, Springer LNCS **11384** (2019) 168–177
84. Hua, R., Huo, Q., Gao, Y., Sun, Y., Shi, F.: Multimodal brain tumor segmentation using cascaded v-nets. BrainLes 2018, Springer LNCS **11384** (2019) 49–60
85. HV, V.: Pre and post processing techniques for brain tumor segmentation. MICCAI BraTS 2018 Pre-proceedings - https://www.cbica.upenn.edu/sbia/Spyridon.Bakas/MICCAI_BraTS/MICCAI_BraTS_2018_proceedings_shortPapers.pdf (2018) 213–221
86. Isensee, F., Kickingereder, P., Wick, W., Bendszus, M., Maier-Hein, K.H.: No new-net. BrainLes 2018, Springer LNCS **11384** (2019) 234–244
87. Islam, M., Jose, V.J.M., Ren, H.: Glioma prognosis: Segmentation of the tumor and survival prediction using shape, geometric and clinical information. BrainLes 2018, Springer LNCS **11384** (2019) 142–153
88. Kao, P.Y., Ngo, T., Zhang, A., Chen, J.W., Manjunath, B.S.: Brain tumor segmentation and tractographic feature extraction from structural mr images for overall survival prediction. BrainLes 2018, Springer LNCS **11384** (2019) 128–141
89. Kermi, A., Mahmoudi, I., Khadir, M.T.: Deep convolutional neural networks using u-net for automatic brain tumor segmentation in multimodal mri volumes. BrainLes 2018, Springer LNCS **11384** (2019) 37–48
90. Kori, A., Soni, M., Pranjal, B., Khened, M., Alex, V., Krishnamurthi, G.: Ensemble of fully convolutional neural network for brain tumor segmentation from magnetic resonance images. BrainLes 2018, Springer LNCS **11384** (2019) 485–496
91. Lachinov, D., Vasiliev, E., Turlapov, V.: Glioma segmentation with cascaded unet. BrainLes 2018, Springer LNCS **11384** (2019) 189–198
92. Lefkovits, S., Szilágyi, L., Lefkovits, L.: Brain tumor segmentation and survival prediction using a cascade of random forests. BrainLes 2018, Springer LNCS **11384** (2019) 334–345
93. Li, X.: Fused u-net for brain tumor segmentation based on multimodal mr images. MICCAI BraTS 2018 Pre-proceedings - https://www.cbica.upenn.edu/sbia/Spyridon.Bakas/MICCAI_BraTS/MICCAI_BraTS_2018_proceedings_shortPapers.pdf (2018) 290–297
94. Liu, M.: Coarse-to-fine deep convolutional neural networks for multi-modality brain tumor semantic segmentation. MICCAI BraTS 2018 Pre-proceedings - https://www.cbica.upenn.edu/sbia/Spyridon.Bakas/MICCAI_BraTS/MICCAI_BraTS_2018_proceedings_shortPapers.pdf (2018) 298–305
95. Ma, J., Yang, X.: Automatic brain tumor segmentation by exploring the multi-modality complementary information and cascaded 3d lightweight cnns. BrainLes 2018, Springer LNCS **11384** (2019) 25–36
96. Marcinkiewicz, M., Nalepa, J., Lorenzo, P.R., Dudzik, W., Mrukwa, G.: Segmenting brain tumors from mri using cascaded multi-modal u-nets. BrainLes 2018, Springer LNCS **11384** (2019) 13–24
97. McKinley, R., Meier, R., Wiest, R.: Ensembles of densely-connected cnns with label-uncertainty for brain tumor segmentation. BrainLes 2018, Springer LNCS **11384** (2019) 456–465
98. Mehta, R., Arbel, T.: 3d u-net for brain tumour segmentation. BrainLes 2018, Springer LNCS **11384** (2019) 254–266
99. Monteiro, M., Oliveira, A.L.: Ensemble of fully convolutional neural networks for brain tumour semantic segmentation. MICCAI BraTS 2018 Pre-proceedings - https://www.cbica.upenn.edu/sbia/Spyridon.Bakas/MICCAI_BraTS/MICCAI_BraTS_2018_proceedings_shortPapers.pdf (2018) 341–348
100. Myronenko, A.: 3d mri brain tumor segmentation using autoencoder regularization. BrainLes 2018, Springer LNCS **11384** (2019) 311–320

101. Nuechterlein, N., Mehta, S.: 3d-espnet with pyramidal refinement for volumetric brain tumor image segmentation. BrainLes 2018, Springer LNCS **11384** (2019) 245–253
102. Popli, A., Agarwal, M., Pillai, G.: Automatic brain tumor segmentation using u-net based 3d fully convolutional network. MICCAI BraTS 2018 Pre-proceedings - https://www.cbica.upenn.edu/sbia/Spyridon.Bakas/MICCAI_BraTS/MICCAI_BraTS_2018_proceedings_shortPapers.pdf (2018) 374–382
103. Puch, S., Sánchez, I., Hernández, A., Piella, G., Prćkovska, V.: Global planar convolutions for improved context aggregation in brain tumor segmentation. BrainLes 2018, Springer LNCS **11384** (2019) 393–405
104. Puybareau, E., Tochon, G., Chazalon, J., Fabrizio, J.: Segmentation of gliomas and prediction of patient overall survival: A simple and fast procedure. BrainLes 2018, Springer LNCS **11384** (2019) 199–209
105. Ren, X., Zhang, L., Shen, D., Wang, Q.: Ensembles of multiple scales, losses and models for brain tumor segmentation and overall survival time prediction task. MICCAI BraTS 2018 Pre-proceedings - https://www.cbica.upenn.edu/sbia/Spyridon.Bakas/MICCAI_BraTS/MICCAI_BraTS_2018_proceedings_shortPapers.pdf (2018) 402–410
106. Rezaei, M., Yang, H., Meinel, C.: voxel-gan: Adversarial framework for learning imbalanced brain tumor segmentation. BrainLes 2018, Springer LNCS **11384** (2019) 321–333
107. Serrano-Rubio, J.P., Everson, R.: Brain tumour segmentation method based on supervoxels and sparse dictionaries. BrainLes 2018, Springer LNCS **11384** (2019) 210–221
108. Shboul, Z.A., Alam, M., Vidyaratne, L., Pei, L., Iftekharuddin, K.M.: Glioblastoma survival prediction. BrainLes 2018, Springer LNCS **11384** (2019) 508–515
109. Shin, H.E., Park, M.S.: Brain tumor segmentation using 2d u-net. MICCAI BraTS 2018 Pre-proceedings - https://www.cbica.upenn.edu/sbia/Spyridon.Bakas/MICCAI_BraTS/MICCAI_BraTS_2018_proceedings_shortPapers.pdf (2018) 428–437
110. Stawiaski, J.: A pretrained densenet encoder for brain tumor segmentation. BrainLes 2018, Springer LNCS **11384** (2019) 105–115
111. Sun, L., Zhang, S., Luo, L.: Tumor segmentation and survival prediction in glioma with deep learning. BrainLes 2018, Springer LNCS **11384** (2019) 83–93
112. Suter, Y., Jungo, A., Rebsamen, M., Knecht, U., Herrmann, E., Wiest, R., Reyes, M.: Deep learning versus classical regression for brain tumor patient survival prediction. BrainLes 2018, Springer LNCS **11384** (2019) 429–440
113. Tseng, K.L., Hsu, W.: End-to-end cascade network for 3d brain tumor segmentation in miccai 2018 brats challenge. MICCAI BraTS 2018 Pre-proceedings - https://www.cbica.upenn.edu/sbia/Spyridon.Bakas/MICCAI_BraTS/MICCAI_BraTS_2018_proceedings_shortPapers.pdf (2018) 466–473
114. Tuan, T.A., Tuan, T.A., Bao, P.T.: Brain tumor segmentation using bit-plane and unet. BrainLes 2018, Springer LNCS **11384** (2019) 466–475
115. Wang, G., Li, W., Ourselin, S., Vercauteren, T.: Automatic brain tumor segmentation using convolutional neural networks with test-time augmentation. BrainLes 2018, Springer LNCS **11384** (2019) 61–72
116. Wang, C.J., Tsai, Y.M., Lee, C., Lee, Y., Costa, A., Hsu, C., Oermann, E., Wang, W.: Brain tumor segmentation with capsule networks versus fully convolutional neural networks. MICCAI BraTS 2018 Pre-proceedings - https://www.cbica.upenn.edu/sbia/Spyridon.Bakas/MICCAI_BraTS/MICCAI_BraTS_2018_proceedings_shortPapers.pdf (2018) 482–491
117. Weninger, L., Rippel, O., Koppers, S., Merhof, D.: Segmentation of brain tumors and patient survival prediction: Methods for the brats 2018 challenge. BrainLes 2018, Springer LNCS **11384** (2019) 3–12
118. Wu, S., Li, H., Guan, Y.: Multimodal brain tumor segmentation using u-net. MICCAI BraTS 2018 Pre-proceedings - https://www.cbica.upenn.edu/sbia/Spyridon.Bakas/MICCAI_BraTS/MICCAI_BraTS_2018_proceedings_shortPapers.pdf (2018) 508–515
119. Xu, P., Hu, Y., Ma, K., Zheng, Y.: A two-step cascaded strategy for automatic brain tumor segmentation in miccai 2018 brats challenge. MICCAI BraTS 2018 Pre-proceedings - https://www.cbica.upenn.edu/sbia/Spyridon.Bakas/MICCAI_BraTS/MICCAI_BraTS_2018_proceedings_shortPapers.pdf (2018) 516–524
120. Xu, X., Kong, X., Sun, G., Lin, F., Cui, X., Sun, S., Wu, Q., Liu, J.: Brain tumor segmentation and survival prediction based on extended u-net model and xgboost. MICCAI BraTS 2018 Pre-proceedings - https://www.cbica.upenn.edu/sbia/Spyridon.Bakas/MICCAI_BraTS/MICCAI_BraTS_2018_proceedings_shortPapers.pdf (2018) 525–533
121. Xu, Y., Gong, M., Fu, H., Tao, D., Zhang, K., Batmanghelich, K.: Multi-scale masked 3-d u-net for brain tumor segmentation. BrainLes 2018, Springer LNCS **11384** (2019) 222–233
122. Yang, H.Y., Yang, J.: Automatic brain tumor segmentation with contour aware residual network and adversarial training. BrainLes 2018, Springer LNCS **11384** (2019) 267–278
123. Yao, H., Zhou, X., Zhang, X.: Automatic segmentation of brain tumor using 3d se-inception networks with residual connections. BrainLes 2018, Springer LNCS **11384** (2019) 346–357
124. Zhang, X., Jian, W., Cheng, K.: 3d dense u-nets for brain tumor segmentation. MICCAI BraTS 2018 Pre-proceedings - https://www.cbica.upenn.edu/sbia/Spyridon.Bakas/MICCAI_BraTS/MICCAI_BraTS_2018_proceedings_shortPapers.pdf (2018) 562–570

125. Zhou, C., Chen, S., Ding, C., Tao, D.: Learning contextual and attentive information for brain tumor segmentation. BrainLes 2018, Springer LNCS **11384** (2019) 497–507
126. Tsuchida, Y., Therasse, P.: Response evaluation criteria in solid tumors (recist): New guidelines. Medical and Pediatric Oncology **37** (2001) 1–3
127. Eisenhauer, E.A., Therasse, P., Bogaerts, J., Schwartz, L.H., Sargent, D., Ford, R., et al.: New response evaluation criteria in solid tumours: revised recist guideline (version 1.1). European journal of cancer **45** (2009) 228–247
128. v. P. van Meerten, E.L., Gelderblom, H., Bloem, J.L.: Recist revised: implications for the radiologist. a review article on the modified recist guideline. European radiology **20** (2010) 1456–1467
129. Ellingson, B.M., Wen, P.Y., Cloughesy, T.F.: Modified criteria for radiographic response assessment in glioblastoma clinical trials. Neurotherapeutics : the journal of the American Society for Experimental NeuroTherapeutics **14** (2017) 307–320
130. Wen, P.Y., Macdonald, D.R., Reardon, D.A., Cloughesy, T.F., Sorensen, A.G., Galanis, E., et al.: Updated response assessment criteria for high-grade gliomas: Response assessment in neuro-oncology working group. Journal of Clinical Oncology **28** (2010) 1963–1972
131. Rutman, A.M., Kuo, M.D.: Radiogenomics: Creating a link between molecular diagnostics and diagnostic imaging. European Journal of Radiology **70** (2009) 232–241
132. Ellingson, B.M.: Radiogenomics and imaging phenotypes in glioblastoma: novel observations and correlation with molecular characteristics. Curr Neurol Neurosci Rep **15** (2015) 506
133. Nicolasjilwan, M., Hu, Y., Yan, C., Meerzaman, D., Holder, C.A., Gutman, D., et al.: Addition of mr imaging features and genetic biomarkers strengthens glioblastoma survival prediction in tcga patients. Journal of Neuroradiology **42** (2015) 212–221
134. Itakura, H., Achrol, A.S., Mitchell, L.A., Loya, J.J., Liu, T., Westbroek, E.M., et al.: Magnetic resonance image features identify glioblastoma phenotypic subtypes with distinct molecular pathway activities. Science Translational Medicine **7** (2015) 303ra128–303ra128
135. Bakas, S., Akbari, H., Pisapia, J., Martinez-Lage, M., Rozycki, M., Rathore, S., et al.: In vivo detection of egfrviii in glioblastoma via perfusion magnetic resonance imaging signature consistent with deep peritumoral infiltration: the ϕ-index. Clinical Cancer Research **23** (2017) 4724–4734
136. Chang, K., Bai, H.X., Zhou, H., Su, C., Bi, W.L., Agbodza, E., et al.: Residual convolutional neural network for the determination of ¡em¿idh¡/em¿ status in low- and high-grade gliomas from mr imaging. Clinical Cancer Research **24** (2018) 1073–1081
137. Akbari, H., Bakas, S., Pisapia, J.M., Nasrallah, M.P., Rozycki, M., Martinez-Lage, M., et al.: In vivo evaluation of egfrviii mutation in primary glioblastoma patients via complex multiparametric mri signature. Neuro-Oncology **20** (2018) 1068–1079
138. Binder, Z.A., Thorne, A.H., Bakas, S., Wileyto, E.P., Bilello, M., Akbari, H., et al.: Epidermal growth factor receptor extracellular domain mutations in glioblastoma present opportunities for clinical imaging and therapeutic development. Cancer Cell **34** (2018) 163–177
139. Havaei, M., Guizard, N., Chapados, N., Bengio, Y.: Hemis: Hetero-modal image segmentation. Cham **2016** (2016) 469–477
140. Ellingson, B.M., Bendszus, M., Boxerman, J., et al.: Consensus recommendations for a standardized brain tumor imaging protocol in clinical trials. Neuro-Oncology **17** (2015) 1188–1198

6 Supplementary Material

6.1 BraTS 2018 Detailed Evaluation

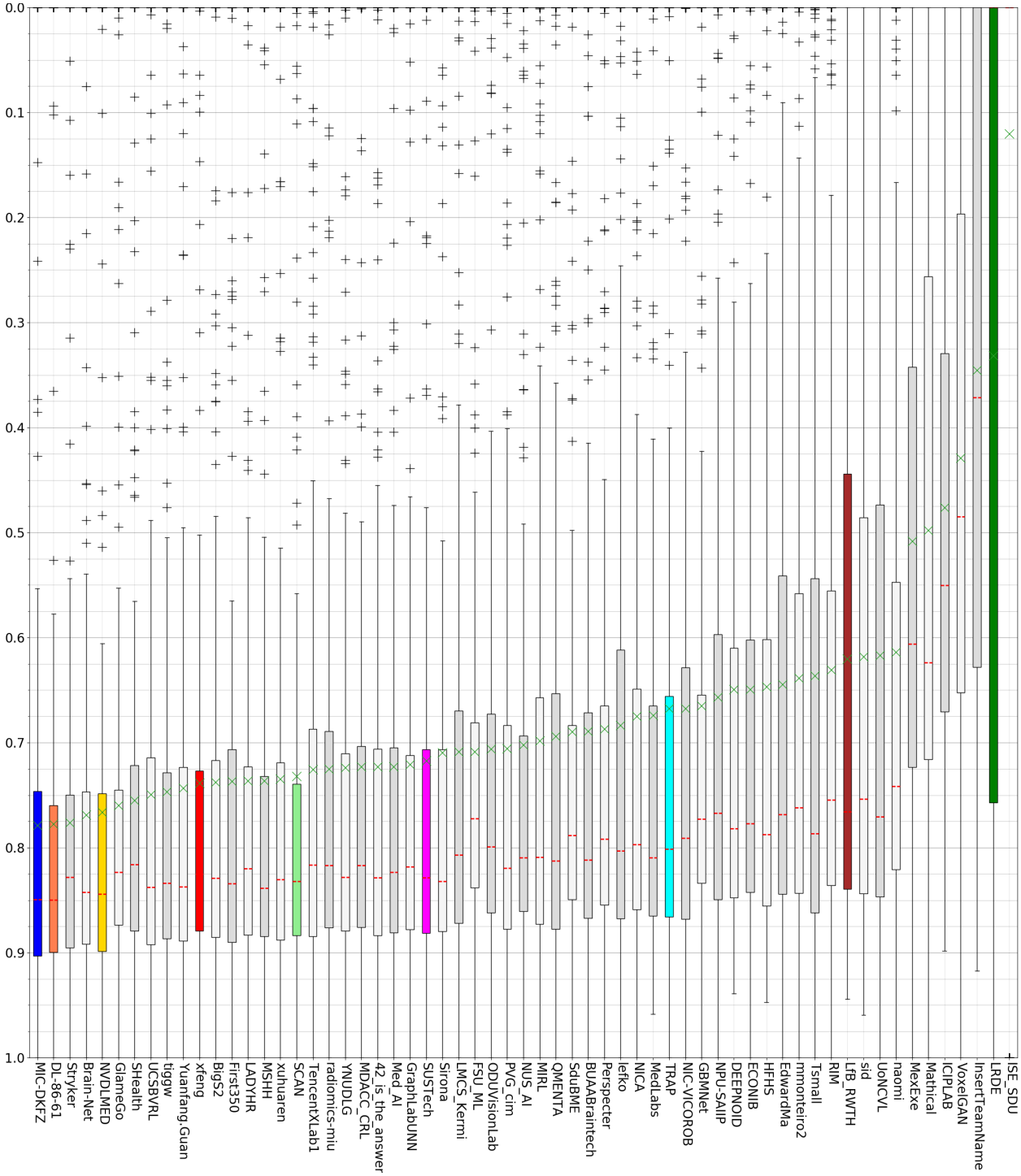

Fig. 9: BraTS 2018 summarizing results (Dice) for the segmentation of the active tumor compartment.

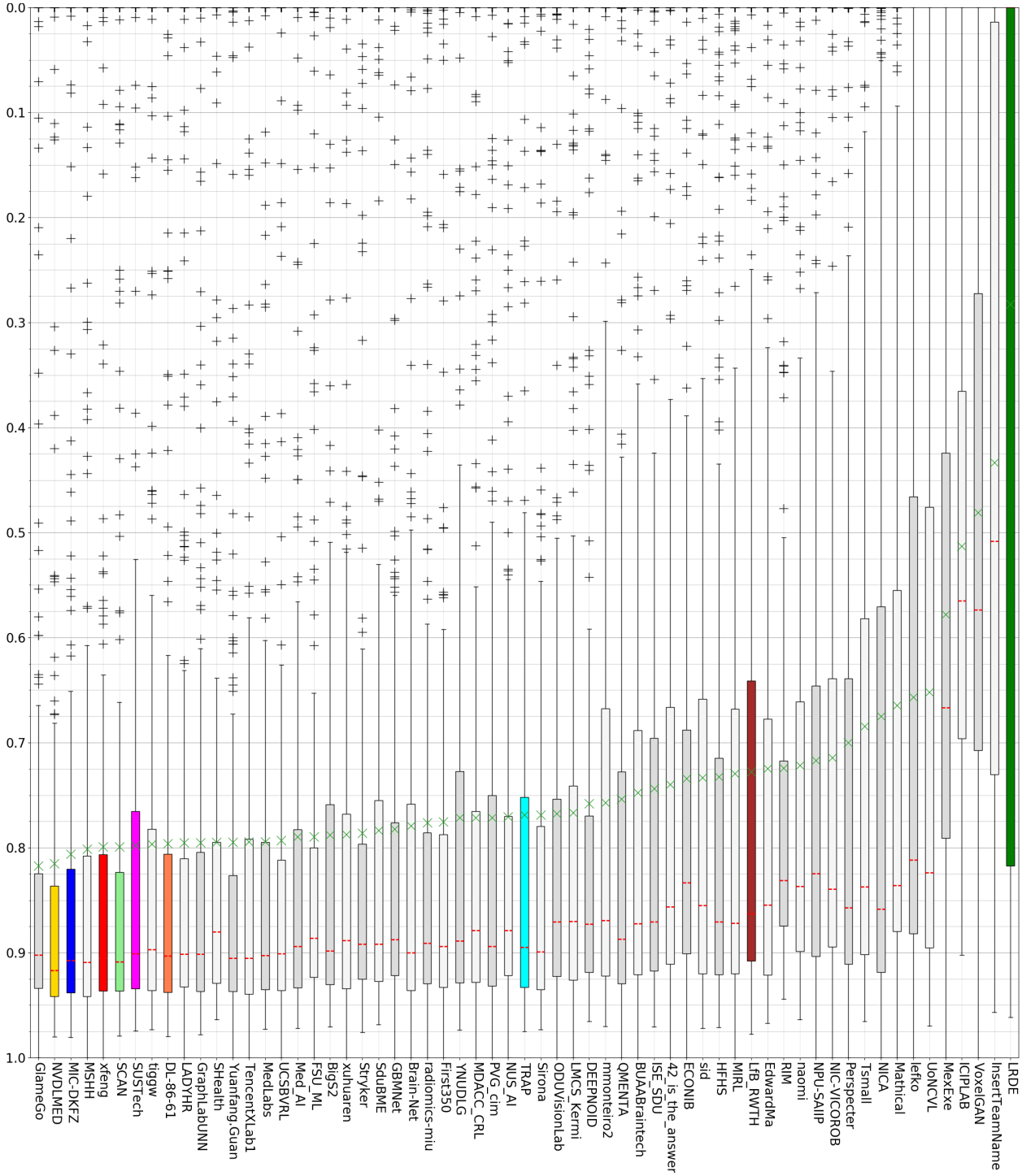

Fig. 10: BraTS 2018 summarizing results (Dice) for the segmentation of the tumor core compartment.

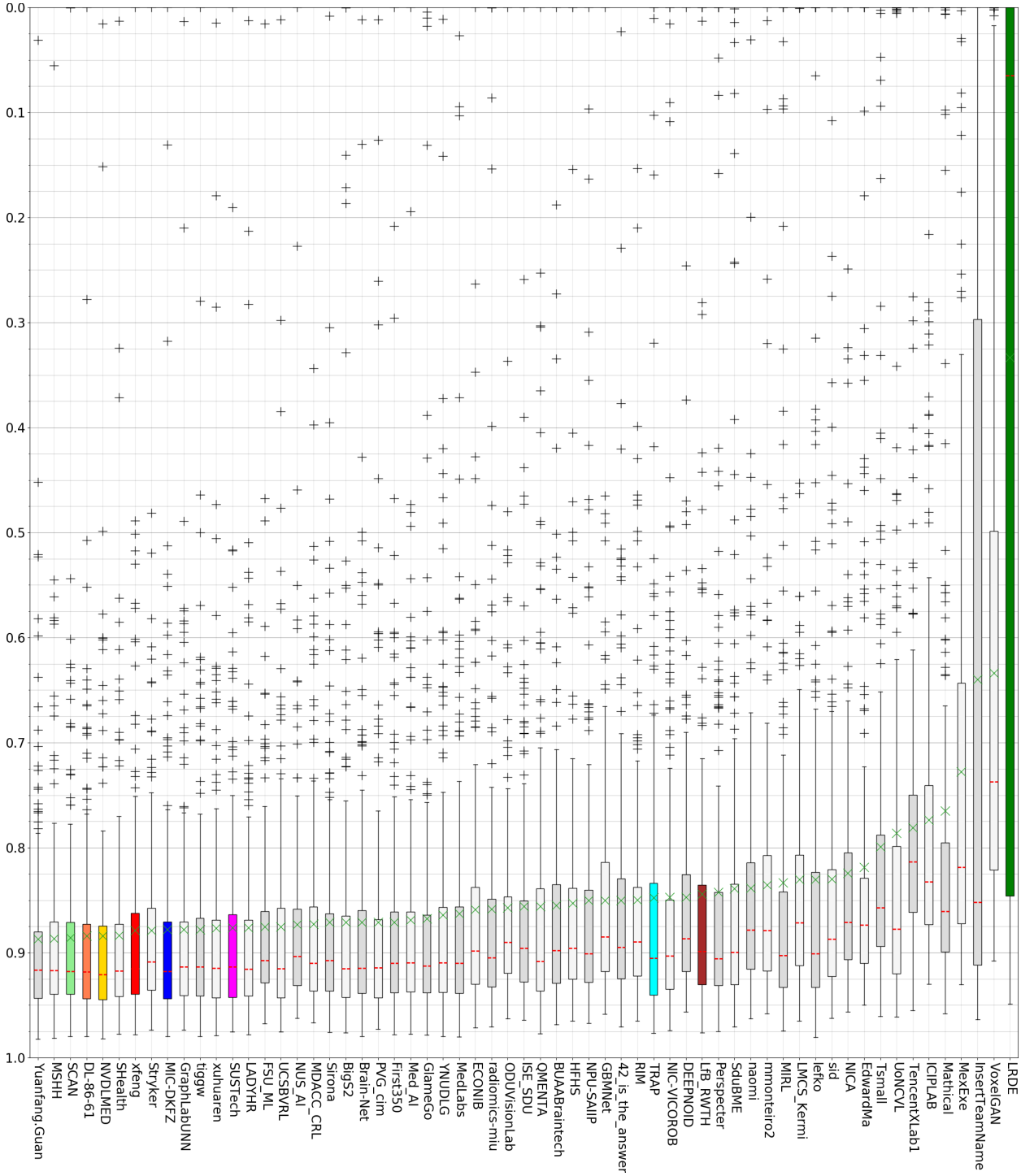

Fig. 11: BraTS 2018 summarizing results (Dice) for the segmentation of the whole tumor compartment.

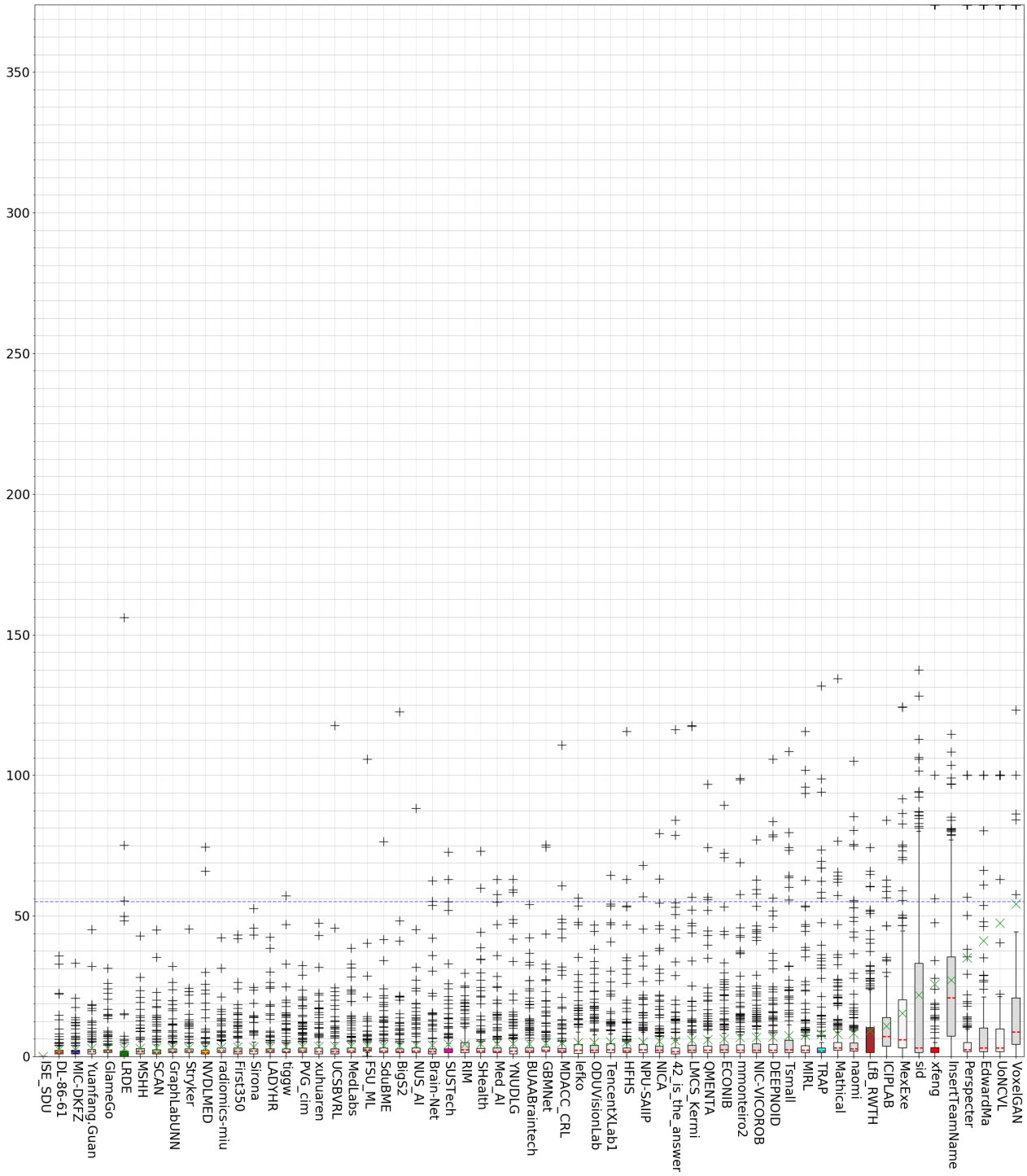

Fig. 12: BraTS 2018 summarizing results (Hausdorff) for the segmentation of the active tumor compartment.

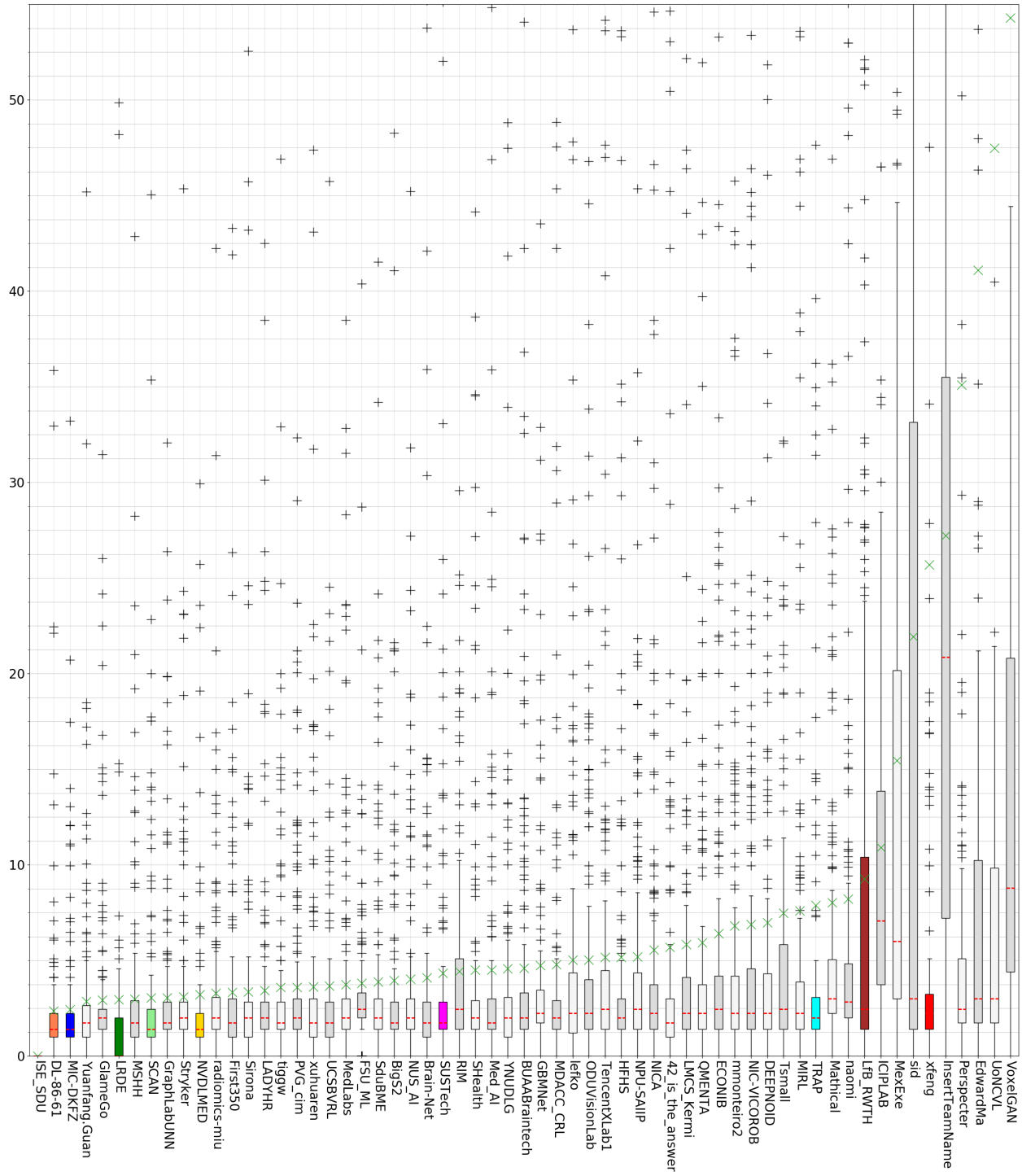

Fig. 13: BraTS 2018 summarizing results (Hausdorff) for the segmentation of the active tumor compartment, with cutoff values for visualization purposes.

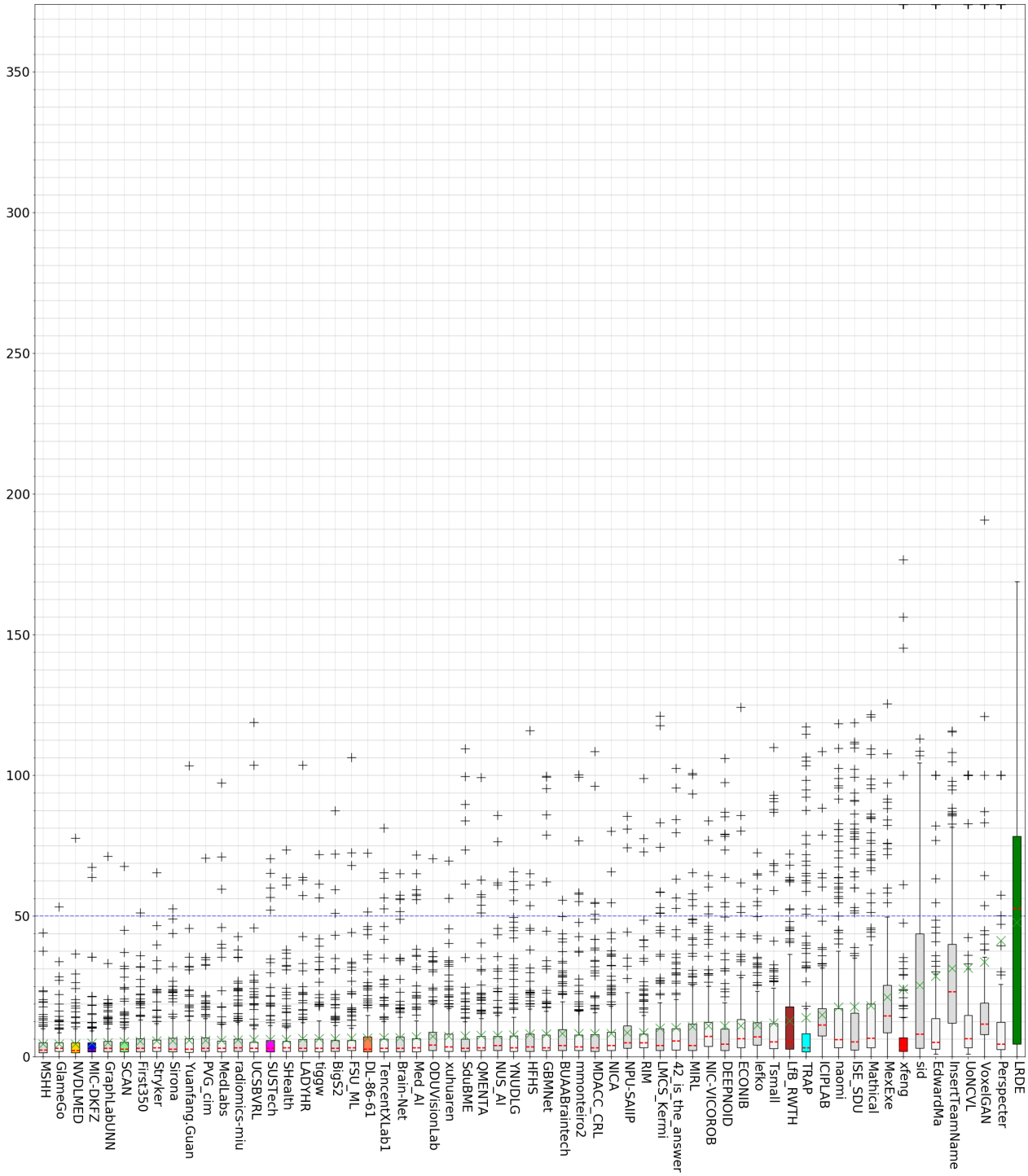

Fig. 14: BraTS 2018 summarizing results (Hausdorff) for the segmentation of the tumor core compartment.

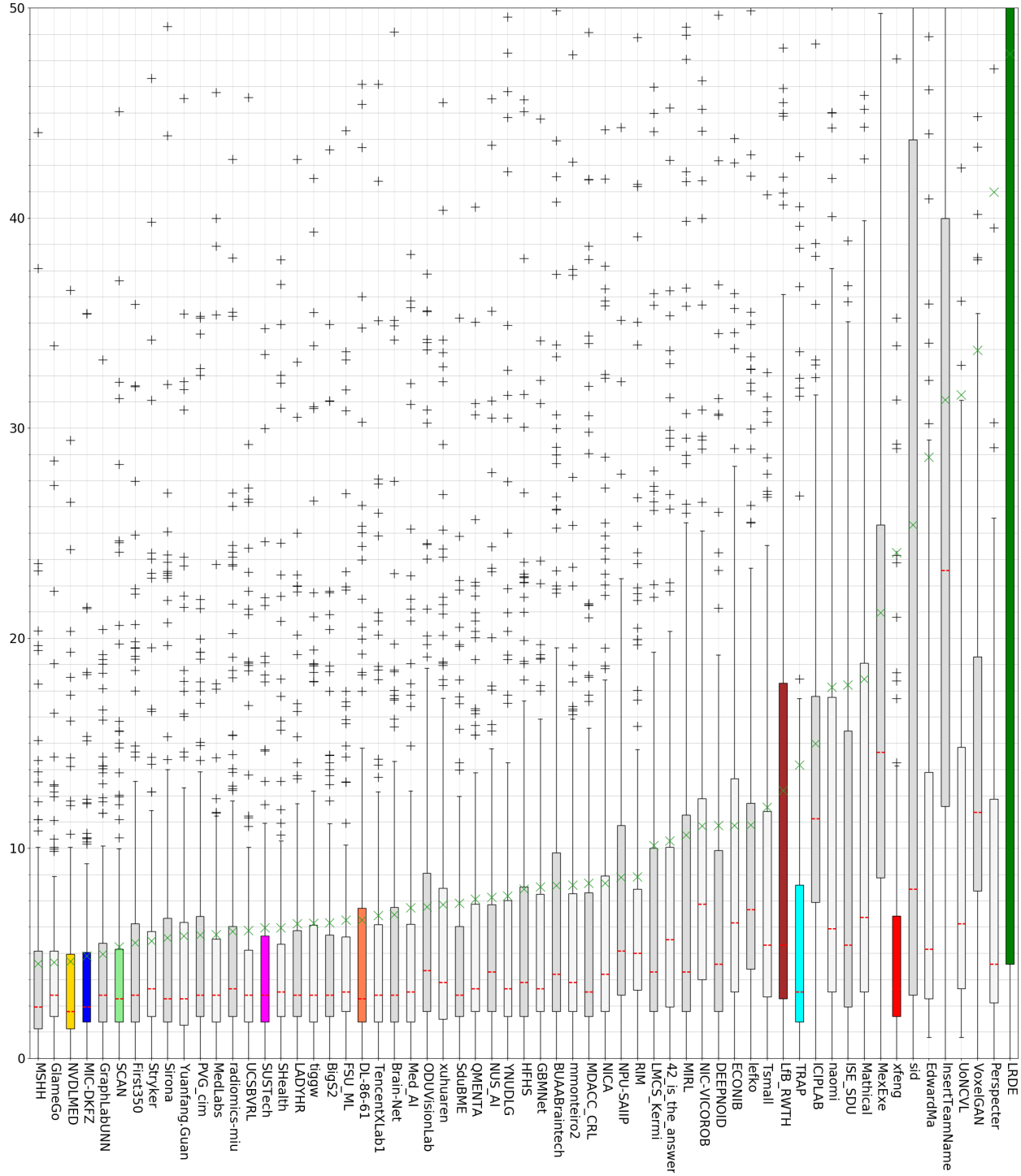

Fig. 15: BraTS 2018 summarizing results (Hausdorff) for the segmentation of the tumor core compartment, with cutoff values for visualization purposes.

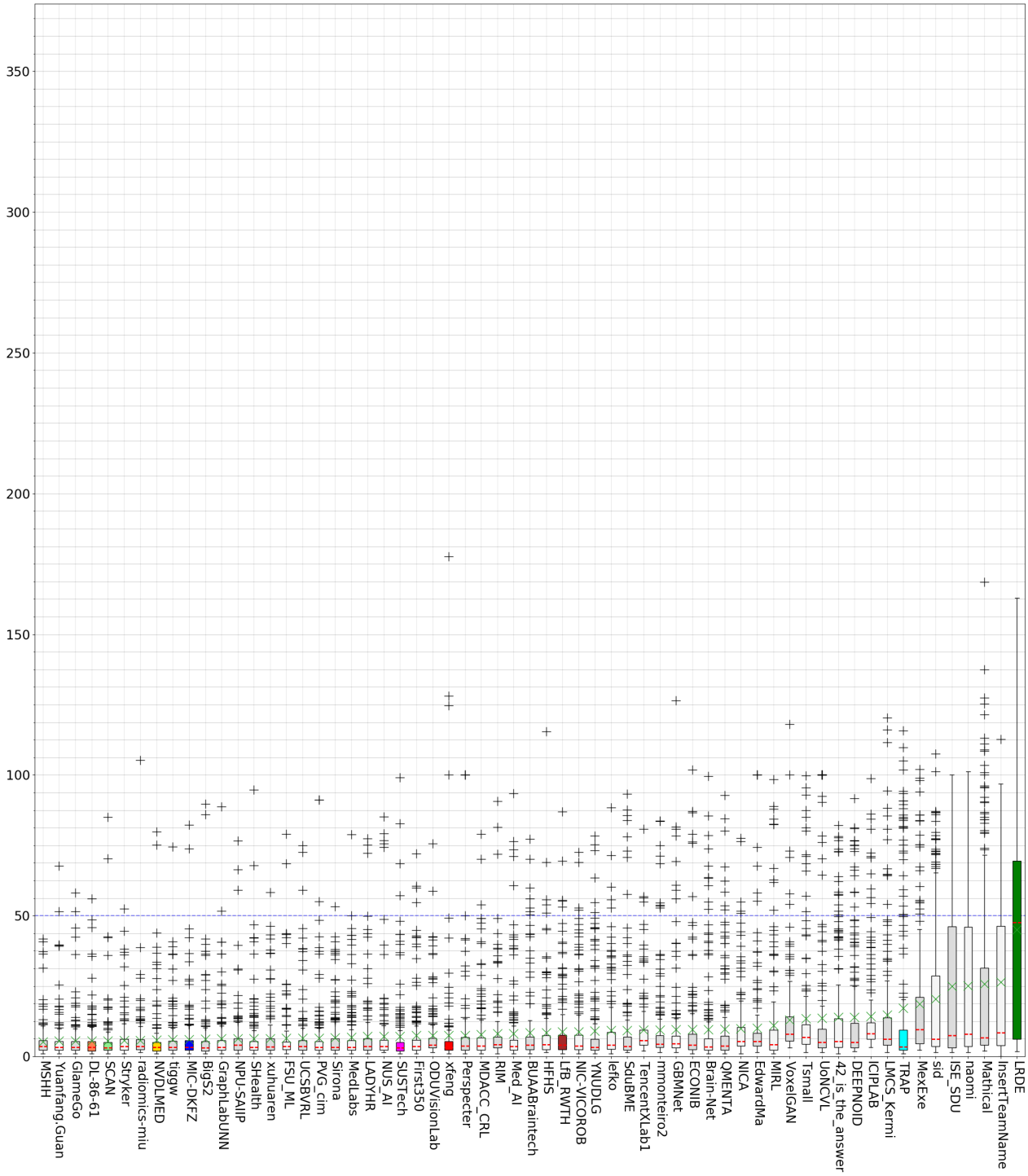

Fig. 16: BraTS 2018 summarizing results (Hausdorff) for the segmentation of the whole tumor compartment.

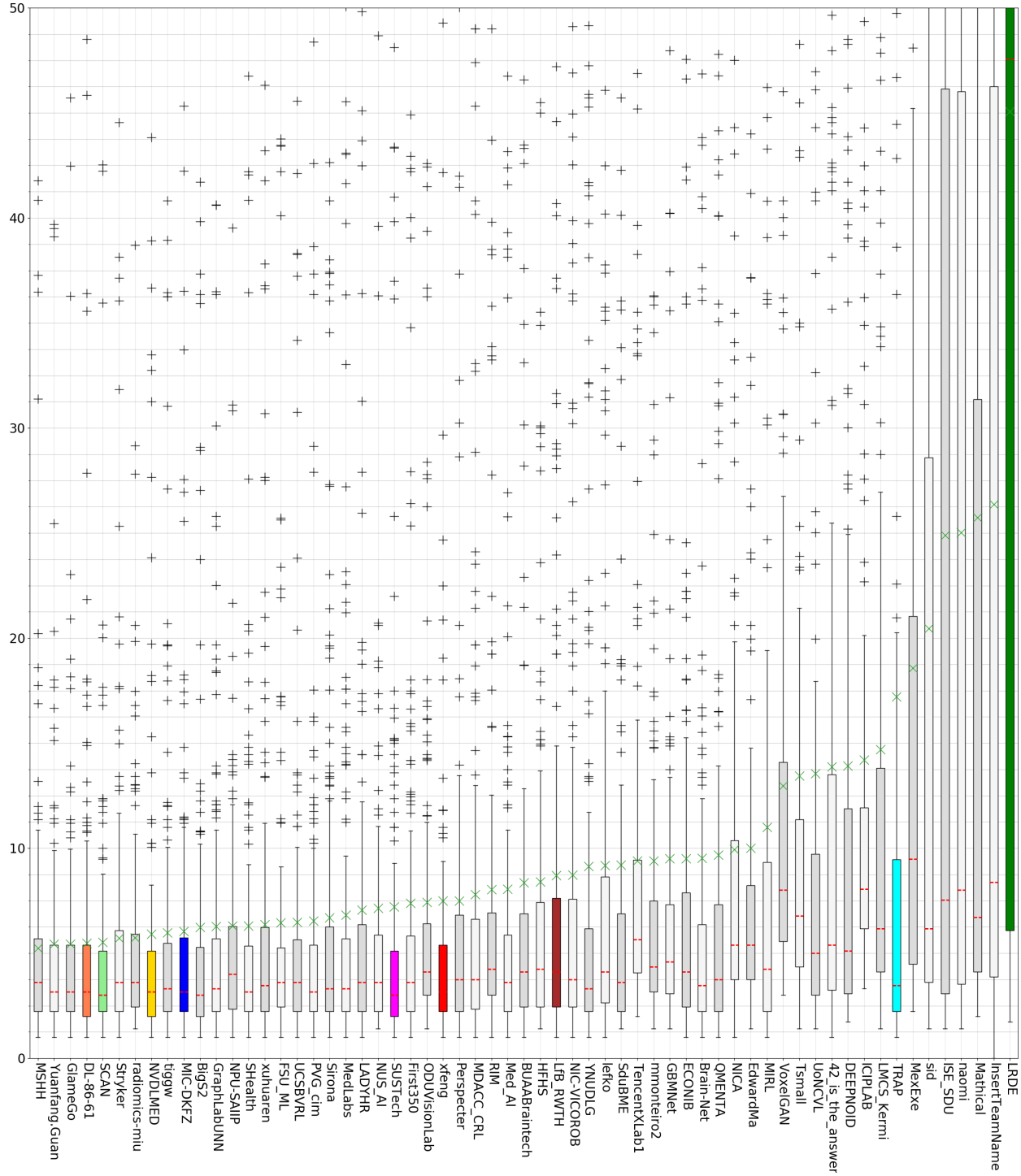

Fig. 17: BraTS 2018 summarizing results (Hausdorff) for the segmentation of the whole tumor compartment, with cutoff values for visualization purposes.

6.2 BraTS 2017 Detailed Evaluation

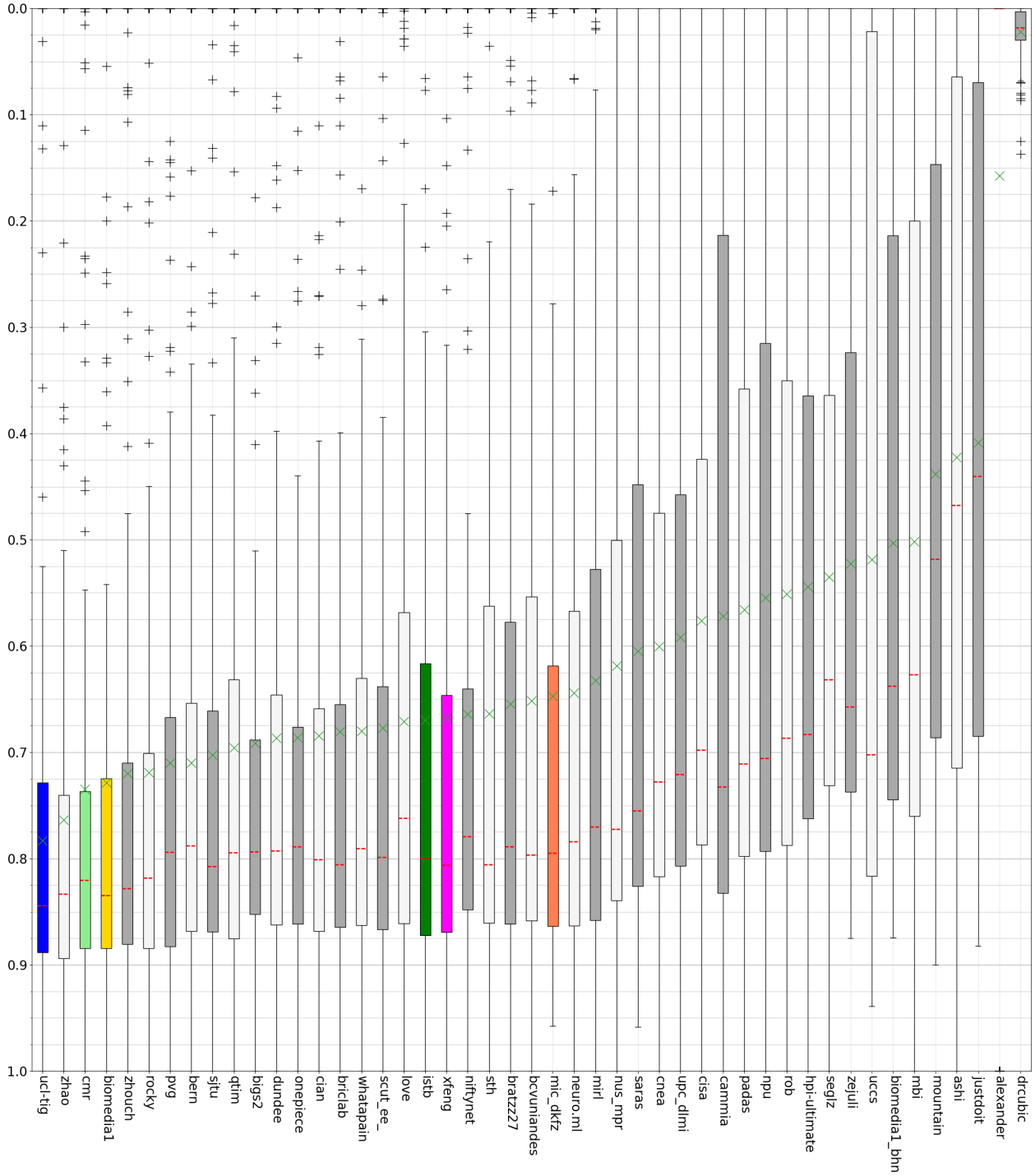

Fig. 18: BraTS 2017 summarizing results (Dice) for the segmentation of the active tumor compartment.

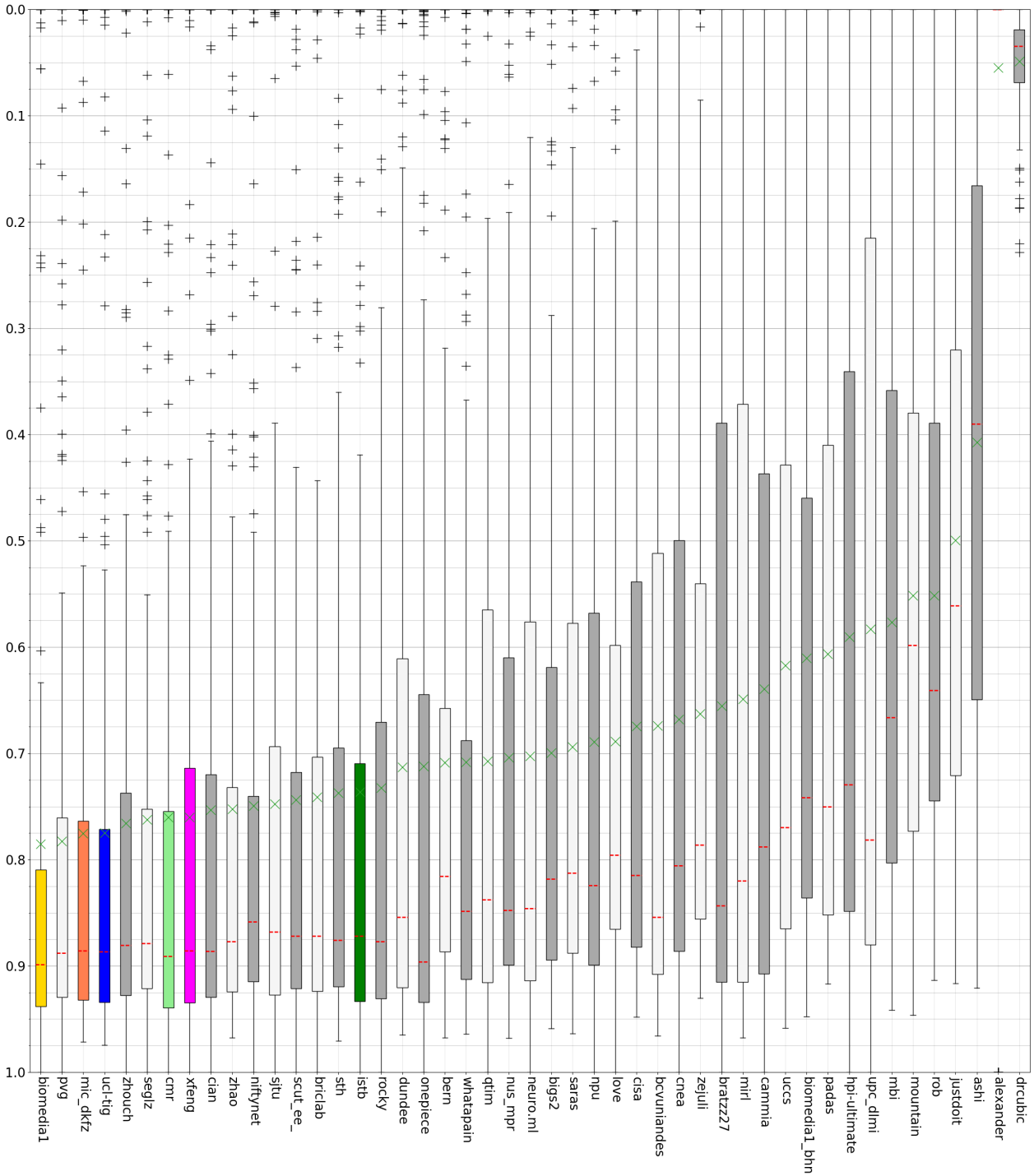

Fig. 19: BraTS 2017 summarizing results (Dice) for the segmentation of the tumor core compartment.

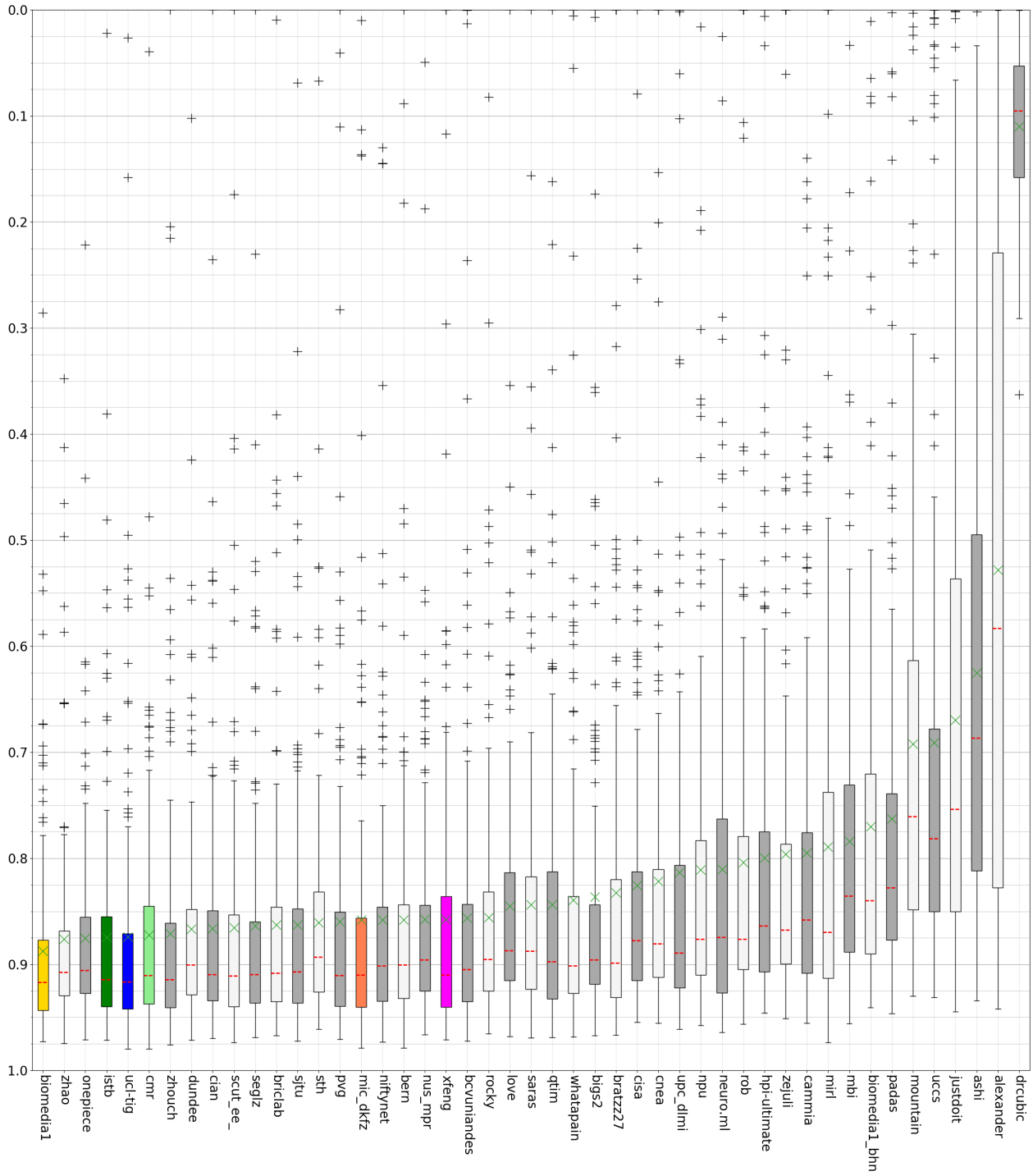

Fig. 20: BraTS 2017 summarizing results (Dice) for the segmentation of the whole tumor compartment.

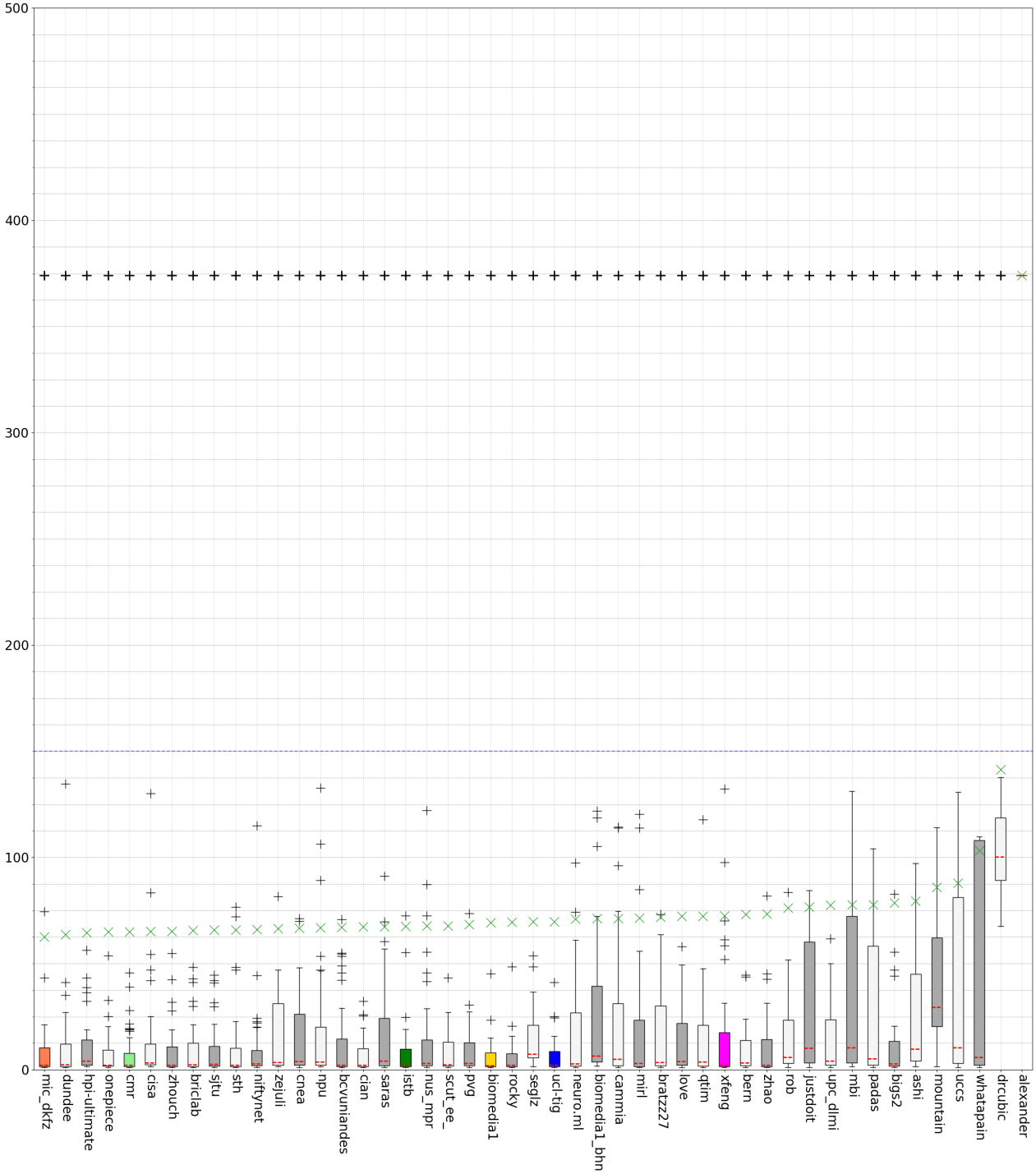

Fig. 21: BraTS 2017 summarizing results (Hausdorff) for the segmentation of the active tumor compartment.

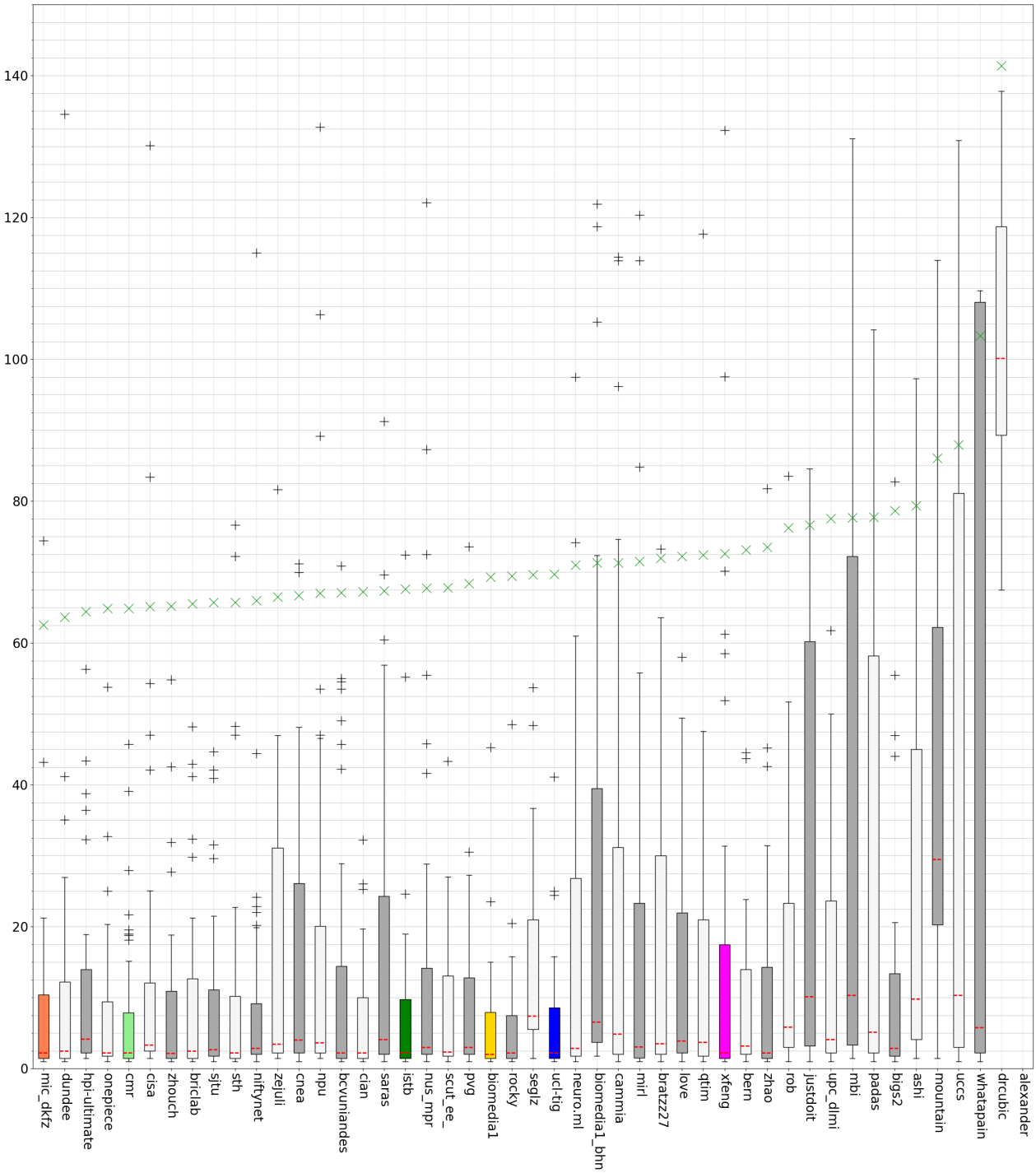

Fig. 22: BraTS 2017 summarizing results (Hausdorff) for the segmentation of the active tumor compartment, with cutoff values for visualization purposes.

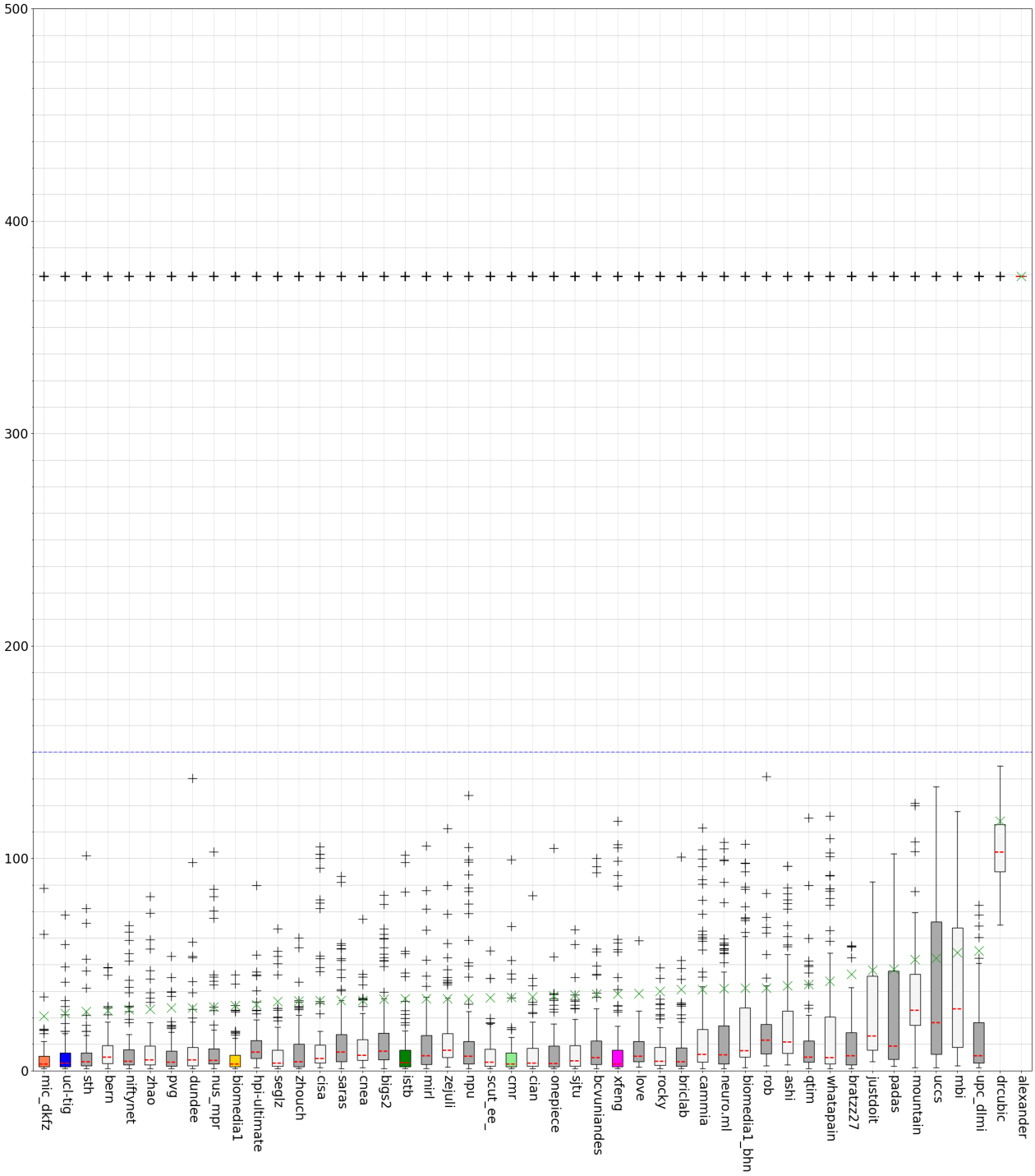

Fig. 23: BraTS 2017 summarizing results (Hausdorff) for the segmentation of the tumor core compartment.

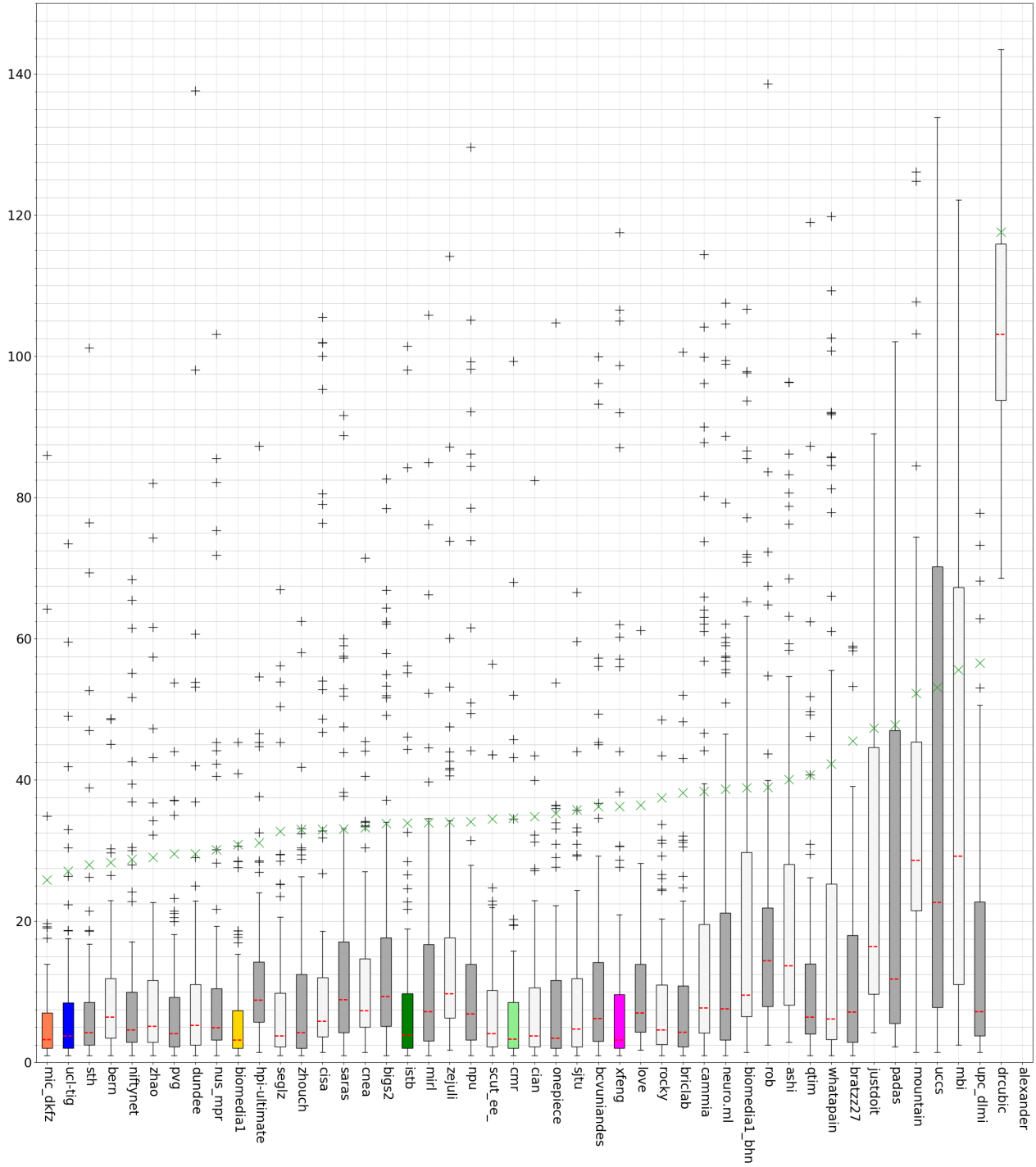

Fig. 24: BraTS 2017 summarizing results (Hausdorff) for the segmentation of the tumor core compartment, with cutoff values for visualization purposes.

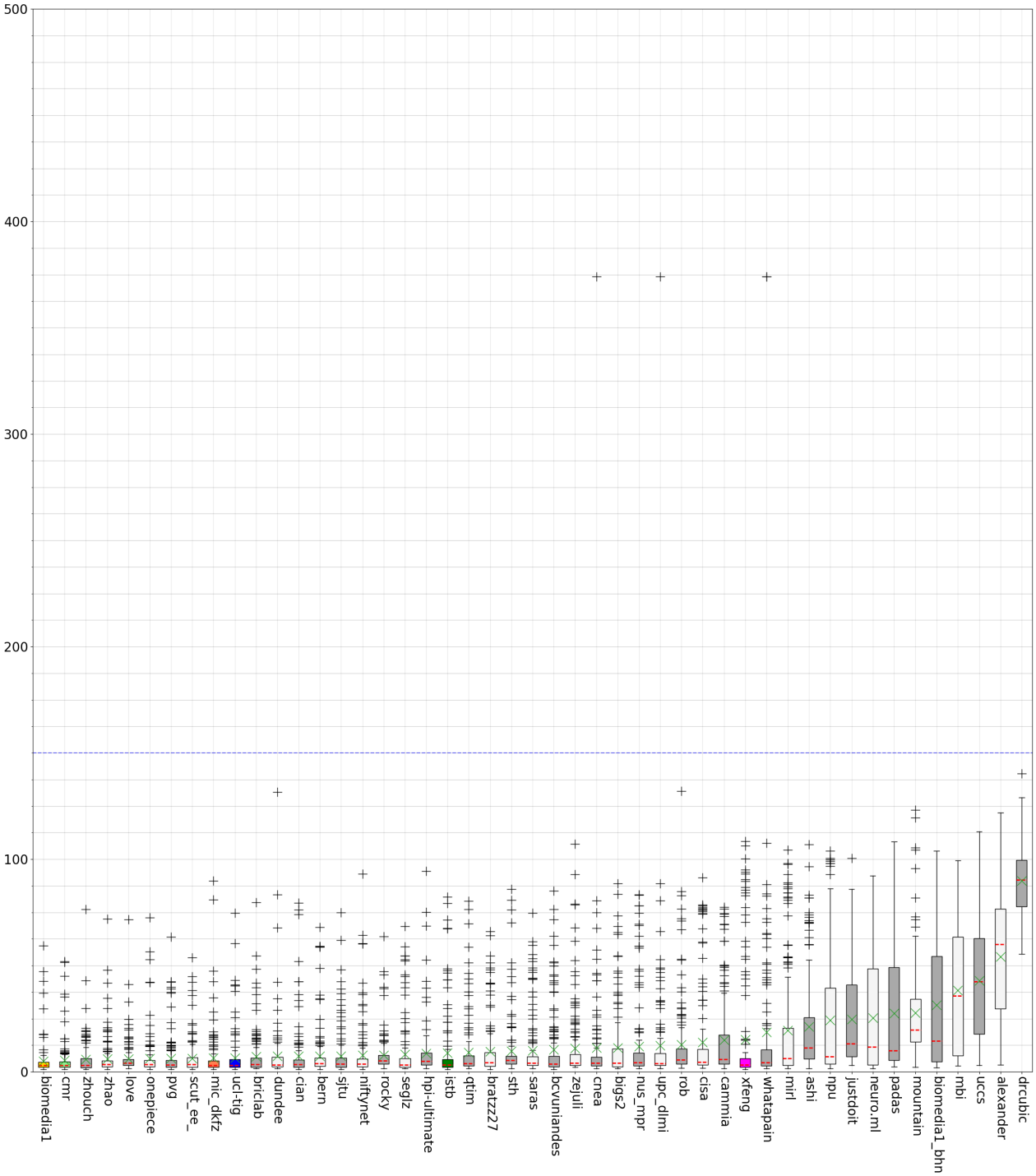

Fig. 25: BraTS 2017 summarizing results (Hausdorff) for the segmentation of the whole tumor compartment.

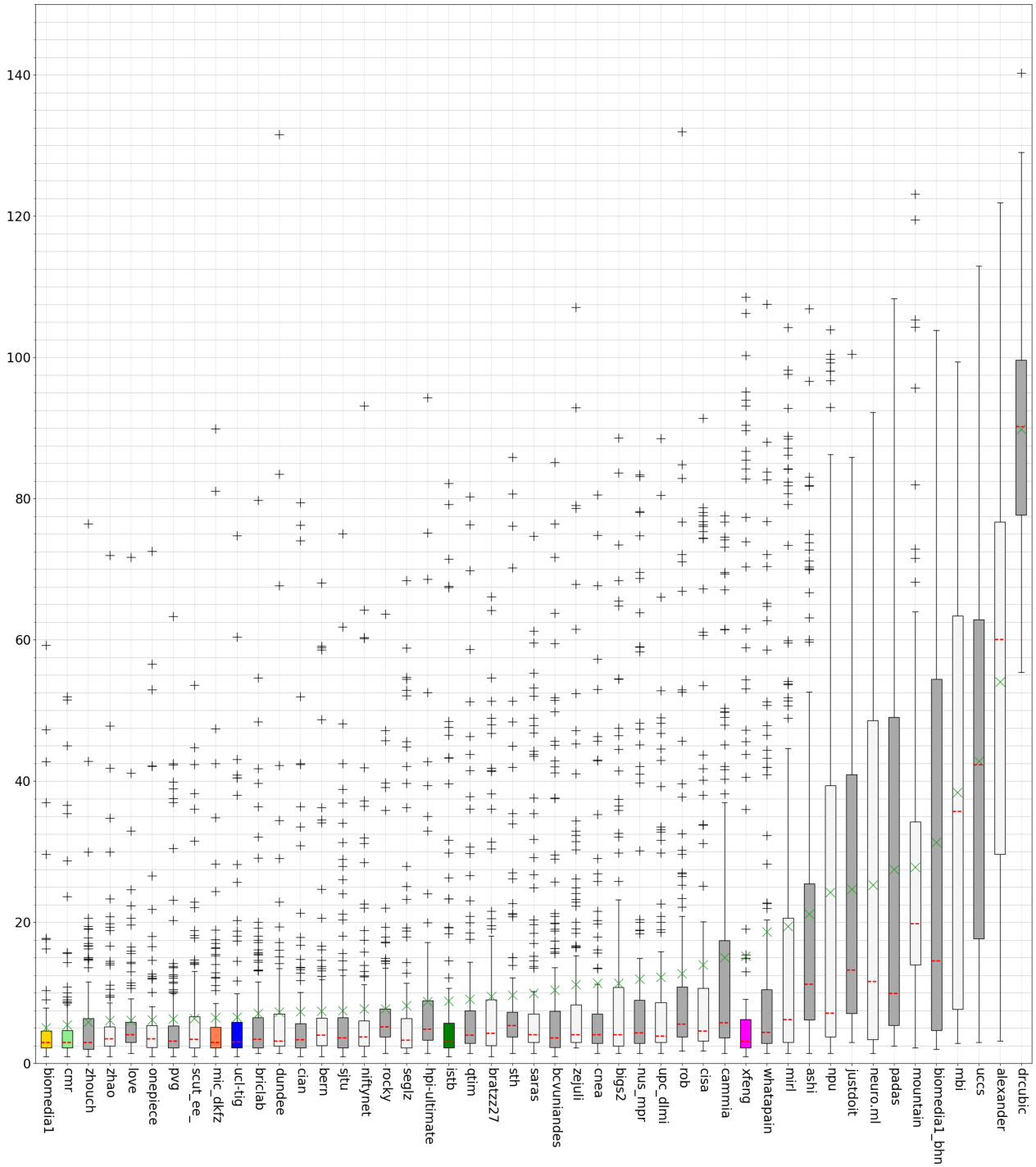

Fig. 26: BraTS 2017 summarizing results (Hausdorff) for the segmentation of the whole tumor compartment, with cutoff values for visualization purposes.